Title
A Climatology of Cutoff Lows and their Precipitation Contributions in the U.S. West Coast

ISBN
9798190939101

Author
Hurley, Kyle

Publication Date
2026-09-15

Peer reviewed|Thesis/dissertation

UNIVERSITY OF CALIFORNIA SAN DIEGO

A Climatology of Cutoff Lows and their Precipitation Contributions in the U.S. West Coast

A Thesis submitted in partial satisfaction of the requirements
for the degree Master of Science

in

Oceanography

by

Kyle Hurley

Committee in charge:

Janet Becker, Co-Chair
Mark Merrifield, Co-Chair
Chris Castellano
Martin Ralph
Zhenhai Zhang

2026

The Thesis of Kyle Hurley is approved, and it is acceptable in quality and form for publication on microfilm and electronically.

University of California San Diego

2026

DEDICATION

I would like to dedicate this project to my loving wife (Sofia), our three beautiful pets (Lily, Graham, and Mocha), and my parents (Brian and Lori). Their support and encouragement are what have led me to continually pursue a career in meteorology, and why I felt that adding my own contribution to science was not only necessary, but required. There have been countless times when my motivation to push forward had run out, and my mental capacity had reached its limit. It was my wife's strong support that led me to this academic avenue we call "Graduate School" in the first place, an arena I never thought I'd see when I graduated from South River High School in 2015. If not for her, I would probably still be living in Virginia, working a boring 9 to 5, with no idea of how my life could have progressed if I had not been motivated to take the first step.

I would also like to dedicate this work to all my sets of loving families: the Hurleys, Andersons, Plackowskis, Cordis, Luzbetaks, Seeleys, Johnsons, and the Heaveys. The lessons they have provided me throughout my life have shaped me into the dedicated man I am today, and I could not be any more appreciative.

TABLE OF CONTENTS

LIST OF FIGURES

LIST OF TABLES

LIST OF ABBREVIATIONS

AR	Atmospheric River
ECMWF	European Centre for Medium-Range Weather Forecasts
ERA5	ECMWF Reanalysis v5
GFS	Global Forecast System
NWS	National Weather Service
NorCal	Northern California
PNW	Pacific Northwest
PRISM	Parameter-elevation Regressions on Independent Slopes Model
R_o	Optimal Radius (Effective Radius)
SoCal	Southern California
USWC	U.S. West Coast
Z	Zulu (Greenwich Mean Time)

ACKNOWLEDGEMENTS

This project could not have been completed without the leadership of the thesis committee, Scripps Institution of Oceanography, and the Center for Western Weather and Water Extremes (CW3E).

I want to sincerely thank Dr. Marty Ralph and the CW3E team for allowing me to commit myself to furthering research that could better understand future impacts of western US weather. Without your approval, guidance, and dedication to this project, my graduate experience would have been relatively short-lived.

I would like to acknowledge Professors Janet Becker and Mark Merrifield, whose dedication to improving the minds of students goes further than many instructors in most fields. Without their support and confidence in my abilities, I potentially never would have been able to accomplish my dreams of earning a Master of Science degree from Scripps Institution of Oceanography. I have come to realize, from many of my current peers, that my committee is truly one in a million, and that each member has gone above and beyond to further my research and prepare my defense.

I would also like to acknowledge Dr. Zhenhai Zhang and Chris Castellano from the CW3E team, whose direct mentorship has allowed me to reach new heights I truly did not know possible. Having the chance to work alongside two highly knowledgeable representatives of the field is a dream come true, and it is through their willingness to take me under their wing that I have made it my personal goal to never let them down.

Through the trials and tribulations this project has presented, I can proudly smile every time I think back to all the work we have accomplished as a team, and look forward to contributing my own pieces to science in the near future. The vast diversity of backgrounds is what makes this team special, and each of your unwillingness to produce nothing but the best outcome possible for me is something I will never take for granted.

Lastly, I would like to acknowledge my wife, Sofia, for without her, none of this would have happened. I never believed I could develop sustainable knowledge within the sciences, yet here I am. At times when I did not believe in myself, she was always there, ready to reassure me of my abilities as a scientist and a loving husband. Through her support throughout my time as a customer service representative, United States Marine, and student, I have been able to achieve the dreams in which I thought were impossible to obtain.

The materials presented are the sole product of hardworking faculty members associated with the University of California San Diego, and the Center for Western Weather and Water Extremes. I would like to recognize and appreciate the review of this paper to Dr. Janet Becker, Chris Castellano, Dr. Mark Merrifield, Dr. Marty Ralph, and Dr. Zhenhai Zhang. Without their support and guidance, this project would have been unable to make the strides it intended. Large portions of this material's data were derived directly from UCSD's MERCED server, which comprised public datasets such as the ECMWF Reanalysis V5 (ERA5) and Parameter-elevation Regressions on Independent Slopes Model (PRISM). Lastly, I would like to thank Kevin Lupo and Ben Moore, whose recent research on the topic helped develop the cutoff low detection method. My thanks also goes to Bin Guan, Duane Waliser, Peter Yao, and Emily Slinskey for the creation and processing of the atmospheric river detection algorithm, which was a necessity for this project to succeed.

VITA

2016 United States Marine Corps Marine Attack Squadron 311

2025 Bachelor of Science in Oceanic and Atmospheric Sciences, University of California San Diego

2026 Master of Science in Oceanography, University of California San Diego

PUBLICATIONS

AMS Fall Meeting 2023, held in San Francisco, CA, 11-15 December 2023, Session: Atmospheric Sciences / Atmospheric River Reconnaissance, Observations, and Forecasts Poster, Poster No. 2413, id. A53L-2413. (Co-Author) (Original Author: Shawn Roj)

ABSTRACT OF THE THESIS

A Climatology of Cutoff Lows and their Precipitation Contributions in the U.S. West Coast

by

Kyle Hurley

Master of Science in Oceanography

University of California San Diego, 2026

Janet Becker, Co-Chair
Mark Merrifield, Co-Chair

A recently developed cutoff low catalog and a long-term precipitation dataset from 1982 to 2024 were analyzed to examine how cutoff lows contribute to annual and seasonal precipitation variability across the U.S. West Coast (USWC) compared to atmospheric rivers (ARs). Assessments were conducted for three regions: Southern California (SoCal), Northern

California (NorCal), and the Pacific Northwest (PNW). On average, 5% of the total precipitation was associated with cutoff lows only, while 48% was associated with ARs only across all three regions. While the relative precipitation contributions from cutoff lows were <5% in the PNW and NorCal, the SoCal region received 9% of its total precipitation from cutoff lows, underscoring their greater importance in SoCal. The PNW and NorCal regions had their peak cutoff low precipitation contributions from May to July, while SoCal's peak was from September to November. Cutoff lows were most frequent in different regions and months, with SoCal having the most frequent landfalling occurrences. The PNW experienced its highest average cutoff low frequencies from January to May, whereas NorCal had its highest average cutoff low frequencies from March to May, and September to November. SoCal's highest average cutoff low frequencies occurred between September and November. While the PNW accounted for the largest total precipitation across the USWC, SoCal had the largest share of precipitation associated with cutoff lows. Precipitation from cutoff lows in SoCal accounted for ~41% of all cutoff low precipitation of the USWC, with the PNW accounting for ~26% and NorCal accounting for ~33%.

Chapter 1 INTRODUCTION

A closed low is a cold-core mid- to upper-tropospheric cyclonic circulation that is surrounded by closed geopotential height contours (Palmén and Newton., 1969). These circulations are often associated with low-pressure systems that create unstable atmospheric conditions conducive to extreme weather events, including tornado outbreaks, heavy precipitation, and flooding (Davies et al., 2006; Parker et al., 2016; Singleton et al., 2007). The center of the low represents the system's minimum geopotential height. These lower geopotential heights do not directly generate vertical motion; however, ascent near closed lows is often produced by dynamical forcing, instability, and upper-level divergence. Closely spaced geopotential height contours in the vicinity of the low's center represent stronger wind velocities, and when combined with a smaller radius of curvature, they indicate stronger relative cyclonic vorticity within these cold-core synoptic features.

A cutoff low is a type of closed low that detaches from the main jet stream flow and is consequently harder to predict in terms of its track, timing, and intensity. Its separation from the main upper-level westerly flow of the jet stream, often near the 250-300 hPa jet level, causes larger uncertainty in the direction of propagation and intensity of this system. Lower geopotential heights at the cutoff low center, stronger geopotential height gradients near the center, and circulation around the cutoff low can affect its intensity, movement, and associated precipitation and wind, posing significant challenges for weather forecasting.

Cutoff lows are a significant source of uncertainty in numerical weather prediction models due to their separation from the main jet stream. Systematic errors in medium-range forecasts of cutoff lows in the National Centers for Environmental Prediction (NCEP) Global Forecast System (GFS) have been previously described as "excessive synoptic progressiveness errors" (Lupo et al. 2023), in which these low-pressure systems are predicted to propagate downstream faster than observed. Observations reveal that some of these cutoff low events are more stationary as they become increasingly separated from the main jet stream. While their predictability in modern GFS versions (v16) has improved (Lupo and Schwartz, 2025), we focus here on developing a better understanding of their contributions to precipitation on the USWC. The USWC has complex topography and diverse climate regimes that contribute to strong spatial variability in precipitation, particularly in Southern California (Dettinger et al., 2011). This precipitation variability poses challenges for local and regional weather prediction offices and for water managers responsible for balancing long-term water supply needs with flood risk mitigation in regions often affected by both droughts and floods. Forecasting a cutoff low to move too quickly through a region can lead to the underestimation of event duration and precipitation impacts, particularly when the system is slow-moving. The ability to distinguish between closed and cutoff lows is important for local and regional meteorologists. Errors in forecasting cutoff lows can contribute to degraded precipitation forecasts and reduced warning lead time for high-impact events, including flooding and infrastructure damage (Lupo and Schwartz, 2025; Lupo et al., 2023; Kasuga et al., 2021).

Cutoff lows tend to be more quasi-stationary, whereas closed lows typically follow the path and orientation of the jet stream over time. The closed low remains influenced by the jet stream's flow and direction, whereas a cutoff low (Figure 2.2, left panel) becomes separated from the main jet stream when upper-level flow is disrupted by planetary/Rossby wave breaking. Rossby wave breaking can generate the absolute vorticity anomalies associated with cutoff low formation (Nadarana and Waugh, 2010; Hoskins et al., 1985). Such planetary wave patterns are often characterized by troughs and ridges. A trough is an elongated region of lower pressure or lower geopotential height, often associated with a southward displacement or deepening of the upper-level flow that can favor colder air, rising motion, and frontal precipitation. A ridge is the opposite: a high-pressure area, associated with warmer temperatures and generally drier conditions. The surrounding trough–ridge pattern can influence the development and movement of a cutoff low, potentially leading to broader downstream changes in the weather pattern over the western United States. While both closed lows and cutoff lows represent low-pressure systems, their orientation relative to the jet stream and their relative size play important roles in steering new and ongoing systems towards the USWC.

While cutoff lows contribute to precipitation over the USWC, it is also important to consider the precipitation contributions of atmospheric rivers (ARs) and their potential interaction with cutoff lows before, during, and after they make landfall. ARs are long and narrow corridors of strong horizontal water vapor transport that are typically associated with a low-level jet stream ahead of the cold front of an extratropical cyclone (Ralph et al., 2018). ARs occur more frequently during the boreal winter months along the USWC and have historically been an important source of precipitation in regions where efficient water management is necessary (Kasuga et al., 2021; Lupo and Schwartz, 2025; Oakley et al., 2014).

Large-scale AR events have historically caused disastrous flooding on the USWC (Corringham et al., 2019), with extreme and exceptional events being the main contributors. The AR Scale of Ralph et al. (2019) assigns a numeric ranking of AR strength at a specific location based on the duration of AR conditions [integrated water vapor transport (IVT) $\geq$250 kg m^{-1} s^{-1}] and maximum IVT during the continuous AR period. The AR Scale provides observers and local forecasters with a framework for communicating the potential impacts of incoming AR events before landfall occurs. AR structure and propagation are closely tied to jet stream orientation and large-scale circulation, whereas cutoff lows detach from the main jet stream and are often characterized as quasi-stationary low-pressure circulations.

Past studies (Ralph et al., 2019; Guan et al., 2015; Guan et al., 2024) have explored the combined effects of cutoff lows and ARs on extreme precipitation events and associated hazards, including flooding, landslides, and infrastructural impacts. In early April 2020, California was affected by an AR and a persistent cutoff low that combined to produce 5–7 inches of rainfall in parts of Southern California, resulting in landslides and flooding. This event resulted in a significant increase in runoff volume in Southern California watersheds during April, in an otherwise relatively dry water year, and persisted for nearly a week (Oakley et al., 2020). Another example of the destructive impacts associated with ARs and cutoff lows was the deadly landslides in Hiroshima, Japan, caused by extreme rainfall in August 2014 that received international attention (Hirota et al., 2015). Together, cutoff lows and ARs can interact and influence atmospheric instability, moisture transport, ascent, precipitation spatial distribution and intensity, and pose challenges for short-to-medium range precipitation forecasting in regions affected by these systems (Hirota et al., 2015).

Prior work on closed lows have focused on building climatologies to better interpret seasonal and regional patterns of these low-pressure systems. Oakley et al. (2013) produced a closed low climatology (1948-2011) for northeastern Pacific Ocean regions to highlight closed lows' landfalling effects, strong interannual variability, and relationship with El Niño Southern Oscillation (ENSO) indices. Yearly time series were created to show periods in which cutoff low event totals increased or declined. Complementing the time series, Oakley et al. (2013) examined the spatial distributions of closed lows and discovered that closed lows produced their largest maximum radius over areas south of NorCal, Nevada, and Arizona regions. Their work followed analytical methods similar to those used in Bell and Bosart (1989), who specifically identified closed lows as synoptic upper-level structures associated with cold-core regions of strong cyclogenesis. Bell and Bosart (1989) examined closed low structures in relation to the main westerly belt that crossed regions from northeast Asia to the northeast U.S. They found that the northeastern Canada region had the highest closed low frequency maximum during late winter, and that the northeastern Pacific exhibited slightly lower total closed low frequency.

Nieto et al. (2005) constructed a 41-year analysis of cutoff lows using three identification criteria: 200 hPa geopotential height minimum, cutoff circulation, and the structure of equivalent thickness and thermal front parameter fields. Ultimately, the study concluded that cutoff low frequencies were underestimated in polar regions but overestimated in subtropical and tropical regions of the Northern Hemisphere. The findings also showed that these cutoff low events had an average lifespan of 2–3 days, with very few exceeding 5 days. These historical studies of closed and cutoff lows are instrumental in understanding how detection methods and behavioral patterns contribute to precipitation in the Northern Hemisphere.

By analyzing ARs and cutoff lows from 1982 to 2024, this study aims to improve our understanding of the contribution of cutoff lows to precipitation over the USWC compared to precipitation due to ARs. The results are examined by season and region to explore variability in cutoff low frequency and associated precipitation. In Chapter 2, we discuss the methods used to detect and catalog cutoff low and AR precipitation used in this study. In Chapter 3, we compare the annual and seasonal cutoff low and AR occurrence frequencies over the USWC and examine the similarities and differences in their temporal and regional patterns. Chapter 4 focuses on the contributions of cutoff lows and ARs to precipitation by season and region. This study extends previous work by providing additional insights into how cutoff lows influence USWC precipitation both regionally and seasonally, with ARs included as an important comparison.

Chapter 2 METHODS

a. Datasets

This study examines cutoff low occurrences using the climatological catalog of Lupo and Schwartz (2025), as well as atmospheric river (AR) occurrences using the AR catalog based on version 4 of the Tracking Atmospheric Rivers Globally as Elongated Targets (tARget) algorithm (Guan and Waliser, 2024) from 1982 to 2024. Both the cutoff low and AR catalogs are based on ECMWF Reanalysis v5 (ERA5; Hersbach et al., 2020). This study also provides estimates of the precipitation associated with both phenomena using Parameter-elevation Regressions on Independent Slopes Model (PRISM) precipitation data (Daly et al., 2008).

Three regions with approximately equal land area were chosen for this study: the Pacific Northwest (PNW), Northern California (NorCal; including the western half of Nevada), and Southern California (SoCal; including much of Arizona). Each region, while geographically connected, exhibits distinct patterns of annual precipitation between cutoff low and AR event occurrences. Previous work has shown that the PNW has a higher AR occurrence frequency than California (Ralph et al., 2019; Dettinger et al., 2011; Collow et al., 2020). By defining regions with similar land areas, regional event frequencies and total precipitation contributions may be compared consistently.

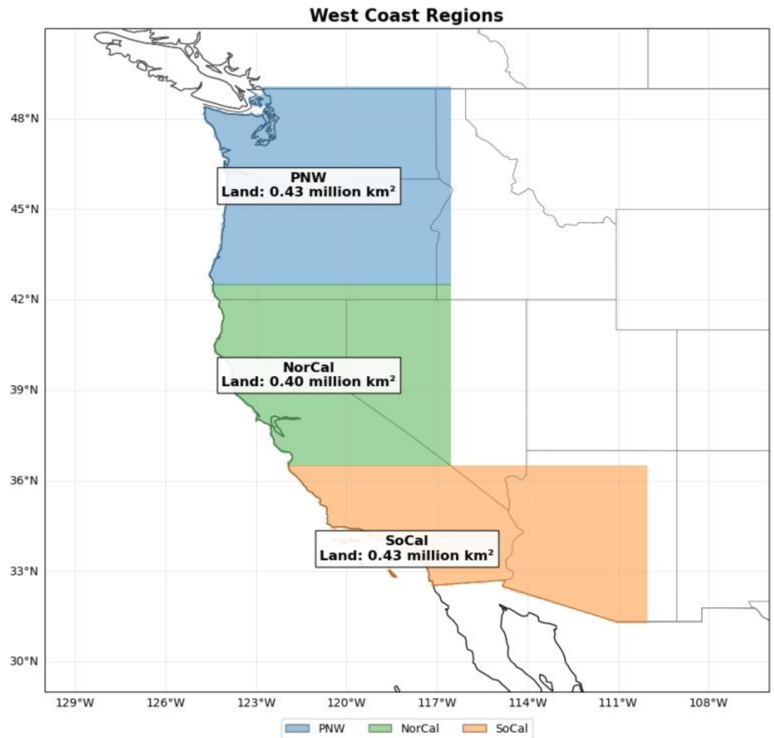

Figure 2.1: Latitudinal and longitudinal constraints applied to three regions. The land area is shown with color shading (blue = PNW; green = NorCal; and orange = SoCal).

Figure 2.1 shows the three domains used to examine AR and cutoff low contributions to precipitation. Splitting the precipitation analysis into three domain sections (PNW, NorCal, and SoCal) helps identify distinct regional precipitation patterns across the USWC. The PNW region contains ~430,340 km^2 of surface area, NorCal approximately ~404,559 km^2 of surface area, and SoCal approximately ~434,566 km^2 of surface area. Total and seasonal mean areal precipitation within each region were calculated by dividing the accumulated precipitation by the region's surface area.

b. Cutoff Low Detection

Cutoff lows have been tracked by Lupo and Schwartz, 2025 utilizing ERA5 500-hPa geopotential height fields. The tracking algorithm is feature-specific, meaning that a cutoff low is well-defined, with criteria that must be met to constitute a cutoff low feature. The features include consistent closed geopotential contours and temporal persistence, as in previous studies (Oakley et al., 2011). These events were tracked using 6-hour timesteps rather than daily to better capture the full amplification and deceleration of these phenomena over time. The centers of these systems were derived using a Point in Polygon (PIP) algorithm that identifies closed geopotential contours and highlights the lowest geopotential heights within the enclosed field. From there, the tracking identifies isolated areas within the 500-hPa fields where the cutoff lows separate from the main westerly flow (jet stream) and do not reconnect while moving upstream along a trough. Temporally, these features must persist for at least 18 hours to be classified as a cutoff low (Oakley et al., 2013). The optimal slope (Kasuga et al., 2021) was used to specify a cutoff low's effective radius. The optimal slope has been defined in past literature as "the height slope of a line intersecting the depression bottom and the nearest tangential point that locally indicates the intensity and scale of an isolated depression" (Kasuga et al., 2021, p. 3119). This definition of the optimal slope accounts for the depth, radius, and slope of the cutoff low to determine its effective range and intensity. A larger optimal slope indicates a stronger geopotential height gradient, meaning stronger geostrophic winds and a stronger cutoff low. Typical effective radii range from 300 to 900 km (Kasuga et al., 2021), with spatial displacement filters applied to detect events that shift by ≥7.5° between 6-hourly timesteps. This filter was crucial for separating fast-moving troughs from cutoff lows.

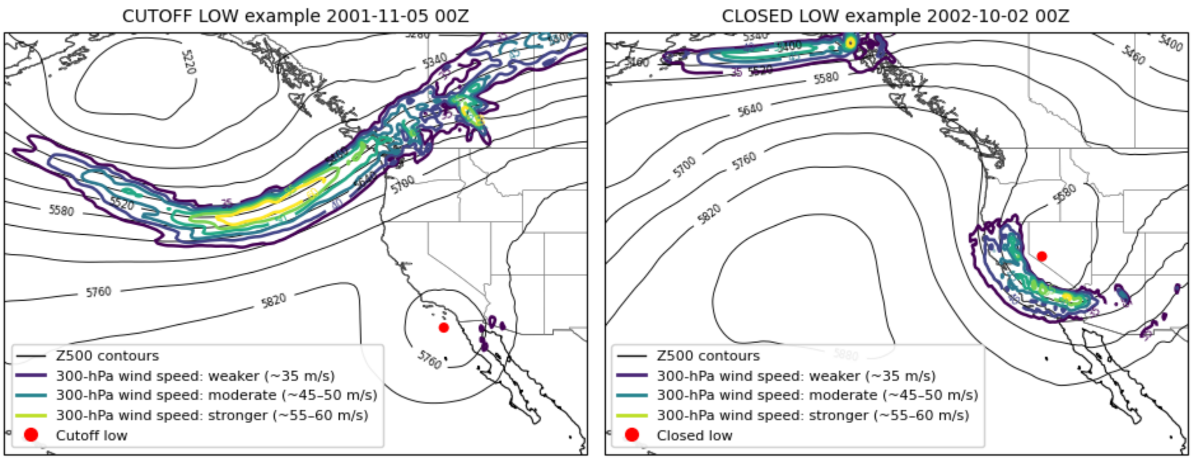

Figure 2.2: Comparison of cutoff low versus closed low identification. This figure shows ERA5 500-hPa geopotential heights (black contours), ERA5 300-hPa wind speed (colored contours), and features identified by the cutoff low detection algorithm. The cutoff low (left) is depicted by the separation of the low's center (red dot) from the main upper-level jet stream. The closed low (right) illustrates how the low-pressure system, while fully closed, remains attached to the overall jet stream system as it propagates downstream.

Figure 2.2 shows a closed low (right) and a cutoff low (left) using ERA5 500-hPa geopotential height fields, with detection methods for closed and cutoff lows developed by Lupo and Schwartz (2025). The detection methods for cutoffs and closed lows were based on the following criteria. First, the centers of these local geopotential height minima must be lower than the surrounding geopotential heights. Second, both systems must have a closed contour surrounding the local minima (Lupo and Schwartz, 2025; Oakley et al., 2013). Finally, a cutoff low is differentiated from a closed low based on whether the system remains connected to the westerly flow and on the low's orientation and direction relative to the jet stream. A low that becomes separated from the westerly flow and equatorward of the main jet stream is classified as a cutoff low (Lupo and Schwartz, 2025).

c. Atmospheric River Detection

Atmospheric river identification was based on version 4 of the tARget catalog (Guan and Waliser, 2015; Guan and Waliser, 2024), which provides 6-hourly detection and tracking of ARs at 00Z, 06Z, 12Z, and 18Z based on ERA5. This catalog identifies AR objects using integrated vapor transport (IVT) and records associated AR characteristics. The detection algorithm utilizes thresholds for poleward orientation, minimum IVT thresholds (>85^{th} percentile of monthly IVT climatology and ≥100 $kg/m^{-1}s^{-1}$), and geometric constraints on length and width

d. Seasonal Occurrence Frequencies

The seasonal absolute frequencies of cutoff lows and ARs in Chapter 3 are calculated by averaging cutoff low and AR occurrences separately over six 2-month periods, starting and ending on the 15th day of each month (15 Jan – 15 Mar, 15 Mar – 15 May, 15 May – 15 July, 15 Jul – 15 Sep, 15 Sep – 15 Nov, and 15 Nov – 15 Jan). The 6-hourly AR and cutoff events are sampled to match the time intervals of the daily PRISM data and to avoid flagging more than one event per day. One daily "hit" was recorded when at least one of the 6-hourly windows featured an AR or cutoff low on a given date. Together, the relative and absolute frequency computations represent data from the cutoff low detection algorithm and the AR detection method, showing how often these events occurred over the studied time period. The total regional precipitation values were found by summing all precipitation volumes within each gridded region. The relative precipitation contributions from cutoff lows, ARs, or both systems at each grid cell are calculated by dividing the AR or cutoff low-specific total precipitation by total precipitation at that grid cell and multiplying by 100.

The absolute occurrence frequencies of ARs and cutoff lows are determined by overlaying all AR and cutoff low grid cells over time across all regions. The seasonal absolute frequencies are calculated using this method but the events are grouped into the previously defined 2-month periods and averaged over time. The relative frequencies (Figure 3.5) were calculated using:

$$R_f = \frac{\#_{ARs} - \#_{Cutoff\ lows}}{\#_{ARs} + \#_{Cutoff\ lows}} \quad where -1 \leq R_f \leq 1 \qquad (1)$$

Values closer to -1.0 represent "cutoff low-dominant" areas and values closer to 1.0 represent "AR-dominant" areas. When the plotted relative frequencies are close to 0.0, the relative frequencies of cutoff lows and ARs are nearly equal. The relative frequency plots enable a direct comparison between cutoff low frequencies and AR frequencies across the climatology period.

Before the analysis of the contribution of cutoff lows and ARs to the precipitation over the USWC, an initial analysis was conducted to understand the dynamical processes associated with cutoff lows and the spatial distribution of precipitation near cutoff lows. We examined how the spatial distribution of precipitation in the vicinity of a cutoff low is related to its effective radius, as defined in recent literature (Kasuga et al., 2021). To achieve this, we divided these radii into four equal quadrants and analyzed the precipitation amounts within each quadrant. It was found that the eastern quadrants (quadrants I and IV; see Figure A.1 in the Appendix) on average contained the largest precipitation totals. This suggests that advection of moist air and forcing for ascent may be enhanced on the eastern or downstream side of these cutoff lows, while the western quadrants experience less favorable conditions for precipitation.

e. Precipitation Categorization

The precipitation analysis is conducted using daily PRISM (Daly et al. 2008) data over the contiguous United States. PRISM daily precipitation values are derived from observational data collected from local NWS stations and partner organizations responsible for rain collection and approximate 24-hour precipitation from 12Z to 12Z. PRISM data is available at 4 km (1/24°) resolution. Monthly total precipitation was calculated from the daily PRISM data to examine seasonal patterns. Daily PRISM precipitation was matched with tracked AR and cutoff low events to classify precipitation into three categories: cutoff low-specific precipitation, AR-specific precipitation, and overlapping precipitation from both ARs and cutoff lows.

Cutoff low contributions to precipitation were estimated using the cutoff low tracking algorithm described earlier in the methods section as well as each cutoff low's "optimal radius" (Kasuga et al., 2021), which is used to approximate the region associated with precipitation from the system itself. The optimal radius component of cutoff low detection was crucial for generating an accurate representation of how cutoff lows over the USWC influence precipitation variability spatially and temporally. Cutoff low-specific precipitation was calculated by summing the total precipitation occurring within a cutoff low's effective radius but outside an AR footprint, whereas AR-specific precipitation was calculated separately as precipitation occurring within an AR footprint but outside a cutoff low's optimal radius. AR precipitation was calculated by summing the total daily accumulated precipitation for each grid cell within an AR footprint based on the AR catalog.

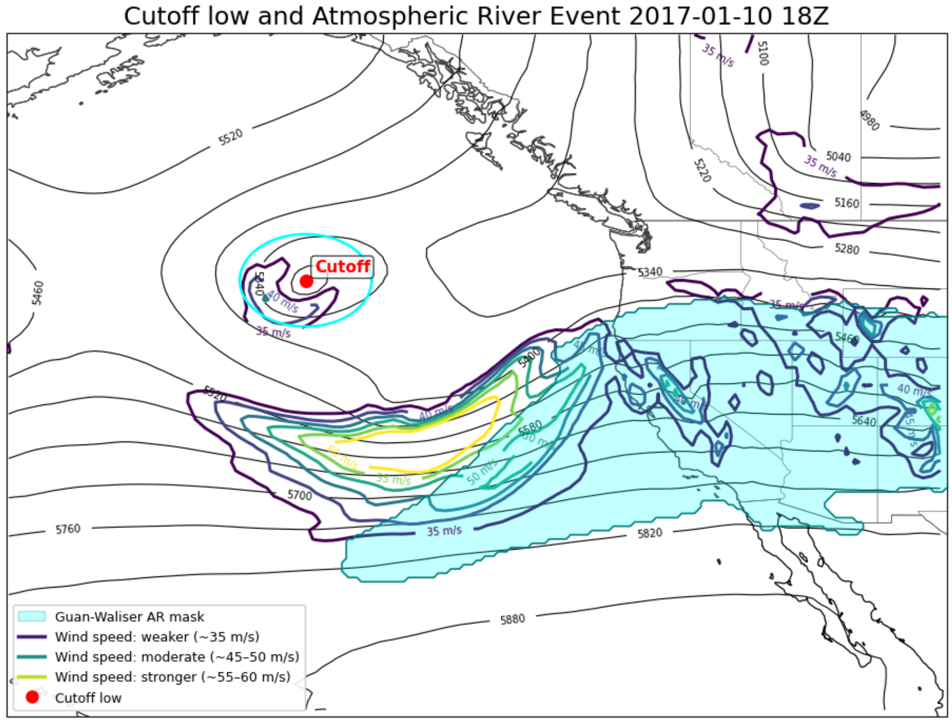

Figure 2.3: A cutoff low near an AR propagating over the USWC. The black contour lines represent the ERA5 500-hPa geopotential heights and the colored contours represent the ERA5 300-hPa wind speeds (m/s). The AR is represented by the Guan-Waliser AR mask (filled cyan shading).

Figure 2.3 illustrates a cutoff low system and an AR. The event of 10 January 2017 at 18Z shows that the cutoff low (red dot) is detached from the upper-level jet stream (colored contours) and the main landfalling AR structure (filled cyan shading) over the USWC.

Chapter 3 CUTOFF LOW AND ATMOSPHERIC RIVER FREQUENCY CLIMATOLOGY OVER THE U.S. WEST COAST

This chapter first examines the climatological frequencies of cutoff lows and ARs to understand their seasonal and regional variability. The individual regions (PNW, NorCal, and SoCal) vary in event-specific frequencies, with AR activity being more frequent in the PNW and NorCal, and landfalling cutoff lows being more frequent in SoCal.

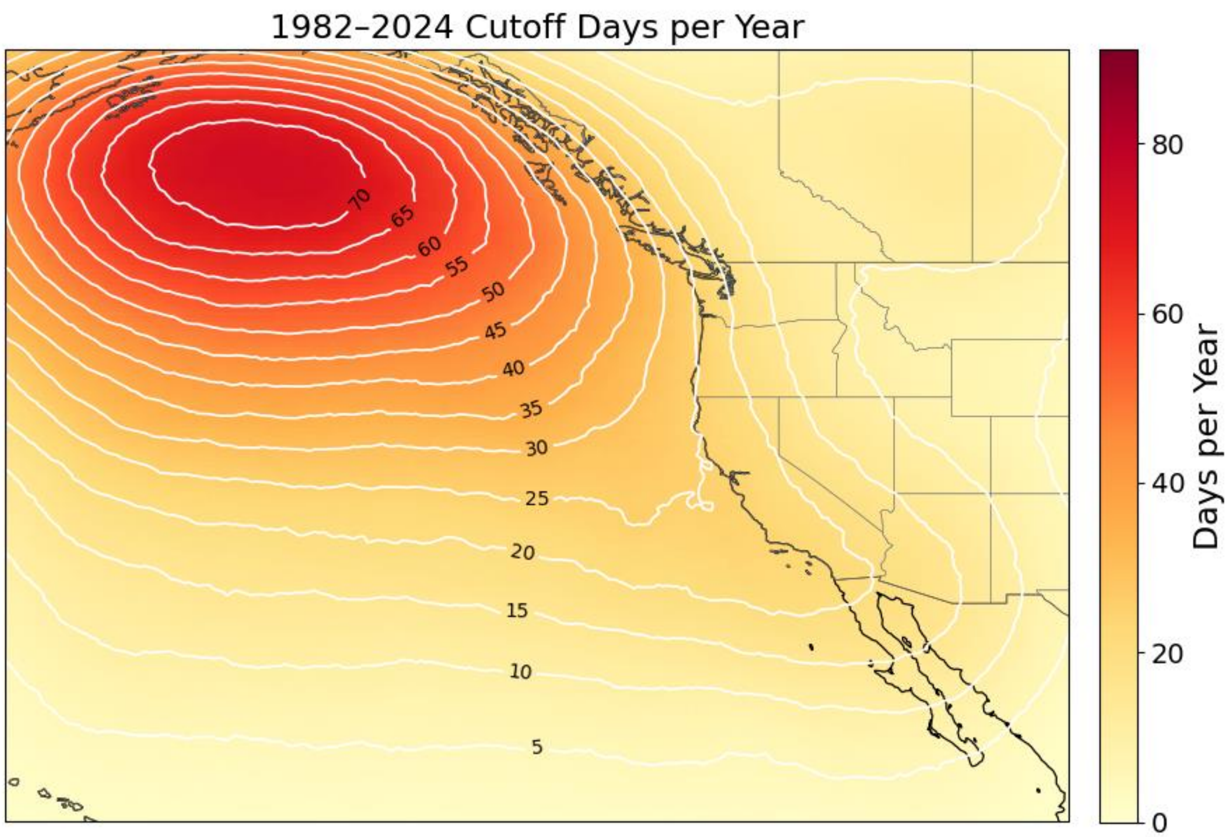

Figure 3.1: Average annual cutoff low frequency (days per year; color shading and white contours) from 1982 to 2024.

3.1 Annual Frequency of Cutoff Lows and ARs

Figure 3.1 illustrates the climatological frequency of cutoff lows over the Northeast Pacific Ocean and western United States. Cutoff lows are most frequent around 51°N latitude and 140°W longitude (over the Gulf of Alaska). Most cutoff lows in this region tend to remain quasi-stationary before weakening and decaying. Others move southeastward along the USWC, associated with deepening trough-like features, and may eventually merge back with the main jet stream (Abatzoglou et al., 2016).

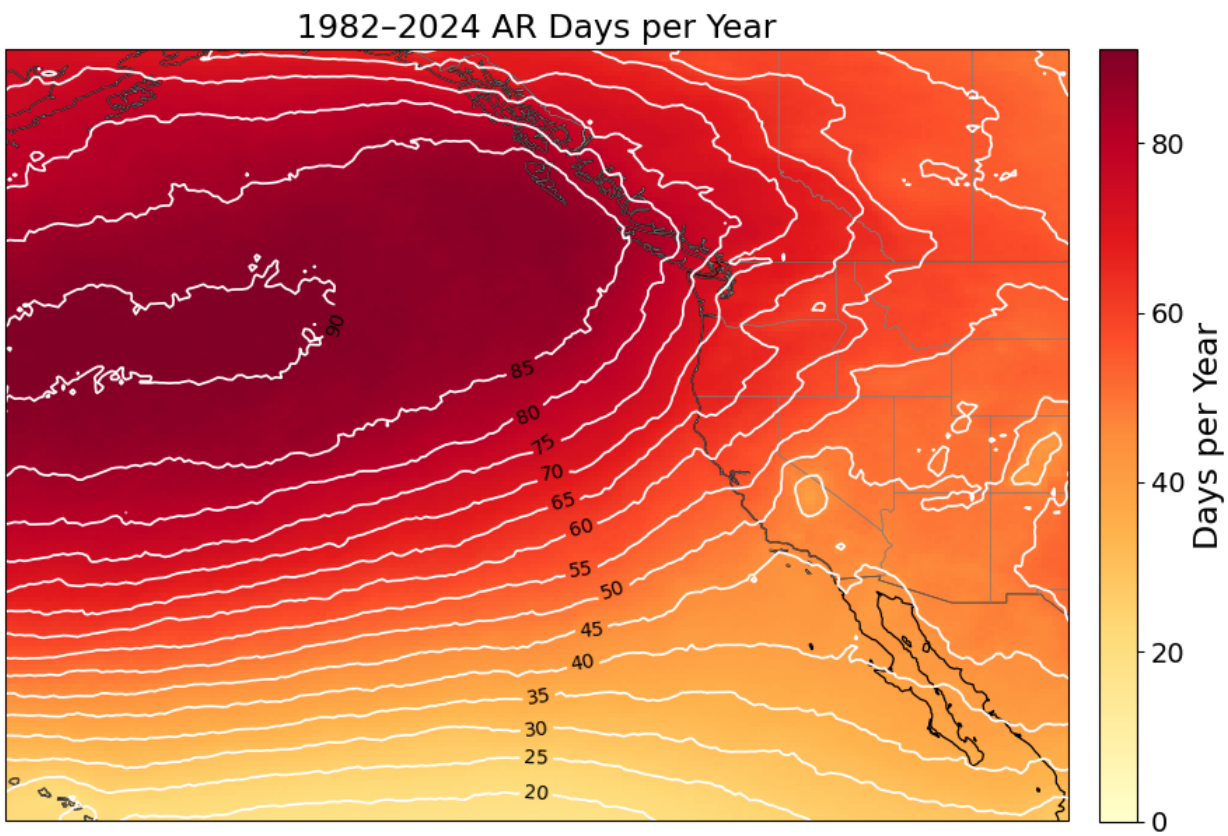

Figure 3.2: Average annual AR frequency (days per year; color shading and white contours) from 1982 to 2024.

AR frequencies peak in areas northwest of coastal PNW ranges (Figure 3.2). The frequency of AR events is higher than cutoff lows over the ocean and land between approximately 51°N and 38°N, with 20–30 more AR days than cutoff low days per year within a given area. AR frequencies exhibit a strong meridional gradient over land, with significantly more occurrences over PNW (65–75 days per year) than over SoCal (45–50 days per year). In general, ARs penetrate further east over the contiguous U.S. than cutoff lows. For total AR events, the stronger frequency gradient occurs near the PNW–NorCal border, where the frequency drops sharply to less than 70 days per year. This highlights the fact that ARs are closely associated with the extratropical cyclones to their north when propagating with the main jet stream (Zhang et al., 2019; Zhang and Ralph, 2021).

3.2 Seasonality of Cutoff Lows and ARs

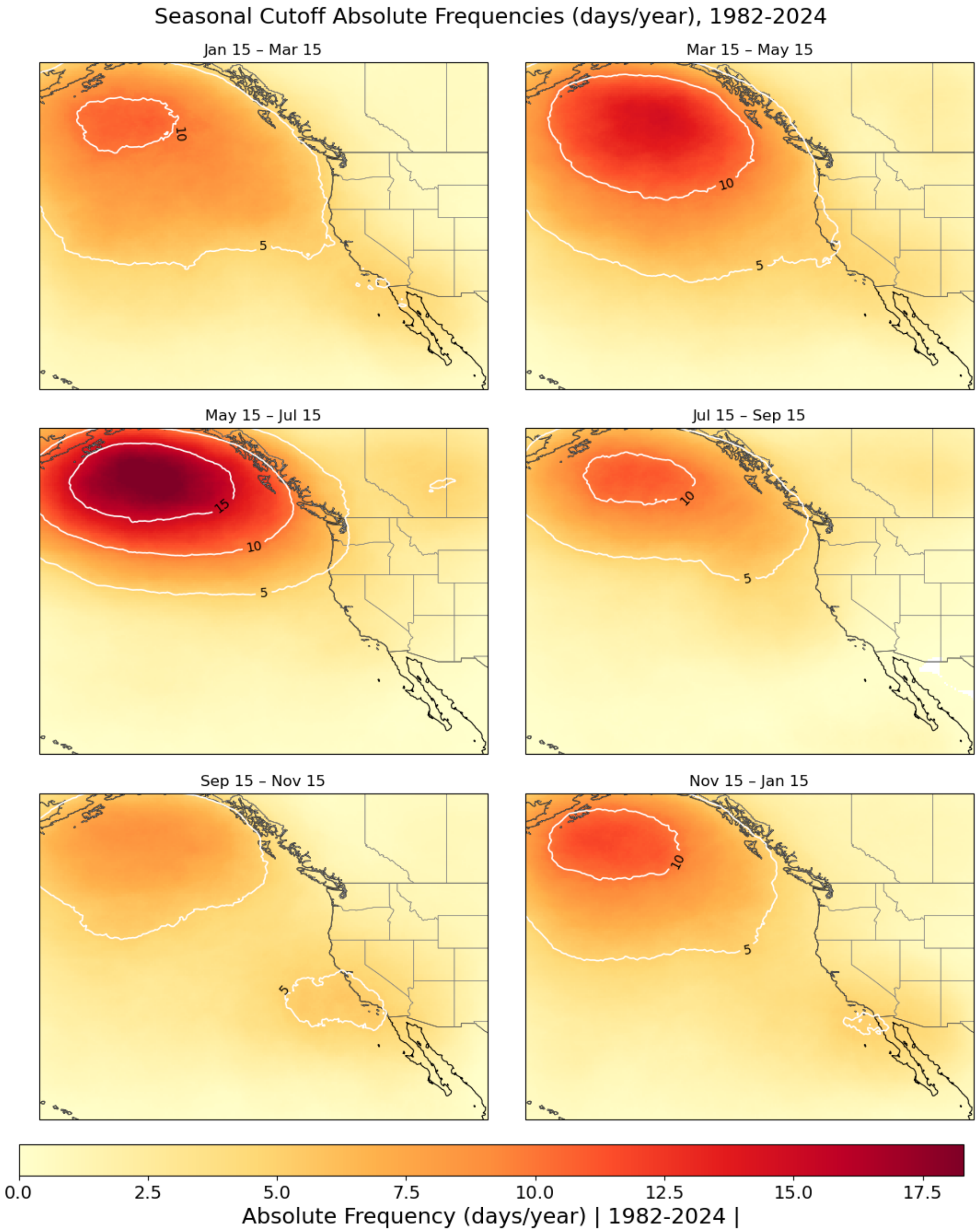

Figure 3.3: Same as Figure 3.1, but for seasonal cutoff low frequency during Jan 15 – Mar 15, Mar 15 – May 15, May 15 – Jul 15, Jul 15 – Sep 15, Sep 15 – Nov 15, Nov 15 – Jan 15.

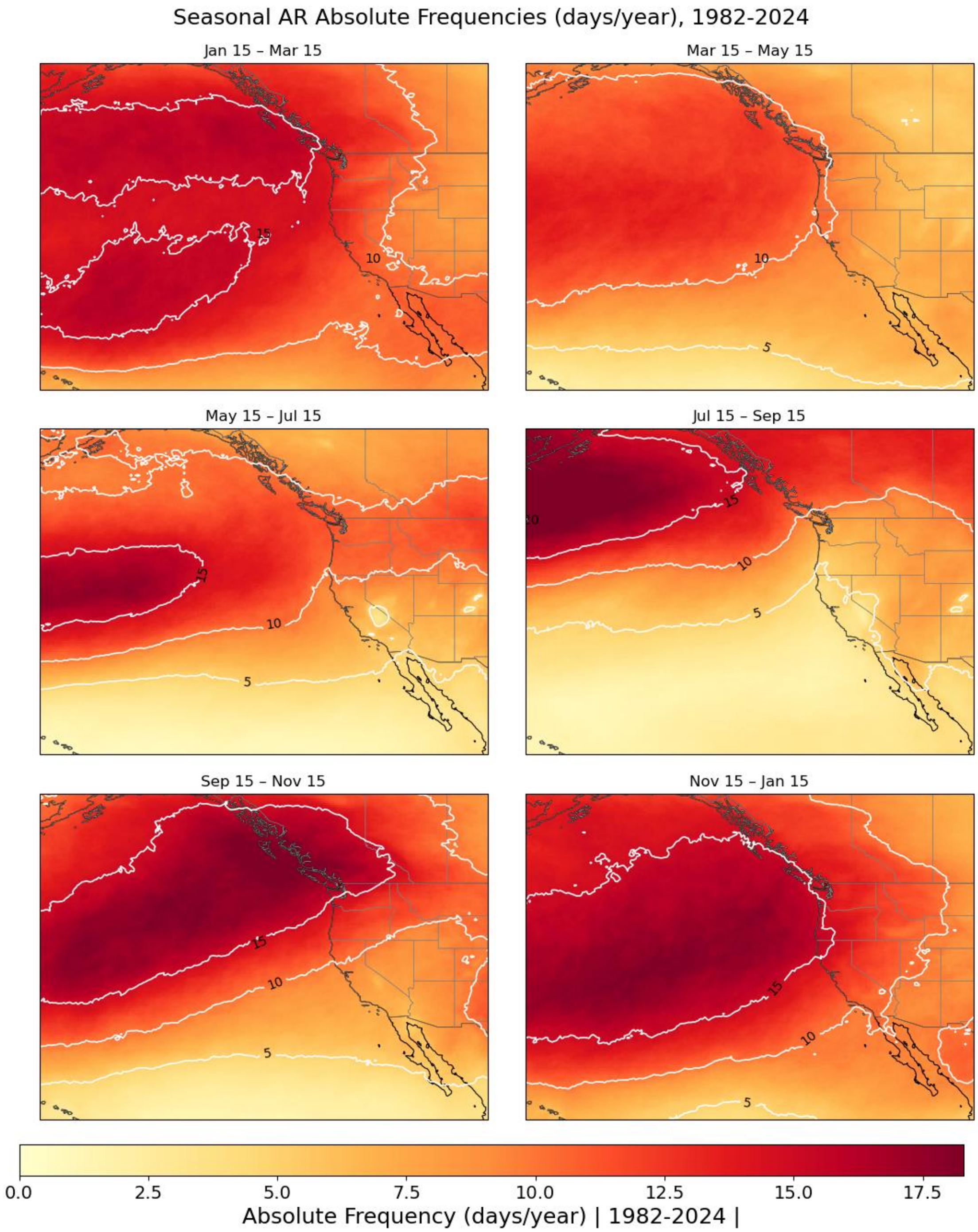

Figure 3.4: Same as Figure 3.2, but for seasonal AR frequency during Jan 15 – Mar 15, Mar 15 – May 15, May 15 – Jul 15, Jul 15 – Sep 15, Sep 15 – Nov 15, Nov 15 – Jan 15.

Cutoff low events dominate from mid-May to mid-July around the Gulf of Alaska region (>15 days per year; Fig. 3.3). This period coincides with the lowest frequency of ARs (~10 days per year) in the same region. One possible reason for the heightened frequency of cutoff lows at this time of year is due to jet stream behavior, as Rossby waves (specifically over the Gulf of Alaska) tend to exhibit wave breaking (Kasuga et al., 2021). These breaking planetary waves can give rise to new closed lows that may eventually become cut off from the main jet stream. Without the jet stream's influence, the cutoff lows will tend to move slowly and exhibit limited displacement (Kasuga et al., 2021). When analyzing individual regions for highest cutoff low frequencies, we found that the highest frequencies in the PNW occurred during mid-May to mid-July. NorCal experienced their highest cutoff low frequencies in mid-March to mid-May, and from mid-September to mid-November. Lastly, SoCal's peaks in cutoff low frequencies extended from mid-September to mid-March.

The strong gradient in AR frequency between the Pacific Ocean and the USWC indicates that many ARs do not make landfall during mid-July to mid-September (Fig. 3.4). Landfalling cutoff lows occur more often later in the year, depending on the region, particularly in SoCal (Fig. 3.3). There is also a large difference in cutoff low event frequencies between different regions from mid-September to mid-January, with SoCal experiencing highest landfalling cutoff low frequencies and the PNW experiencing the lowest. In contrast, ARs are consistently more frequent in PNW and NorCal than in SoCal across all months. Together, figures 3.1 and 3.3 show that these cutoff lows tend to propagate southeastward, starting from the Gulf of Alaska, and migrating toward SoCal. Cutoff lows from mid-March to mid-May and mid-May to mid-July, seem to reach their maximum frequencies around the Gulf of Alaska. All other months see less centralized frequencies around the Gulf of Alaska, and instead, represent more southerly migration along the USWC.

3.3 Relative Frequency of Cutoff Lows and ARs

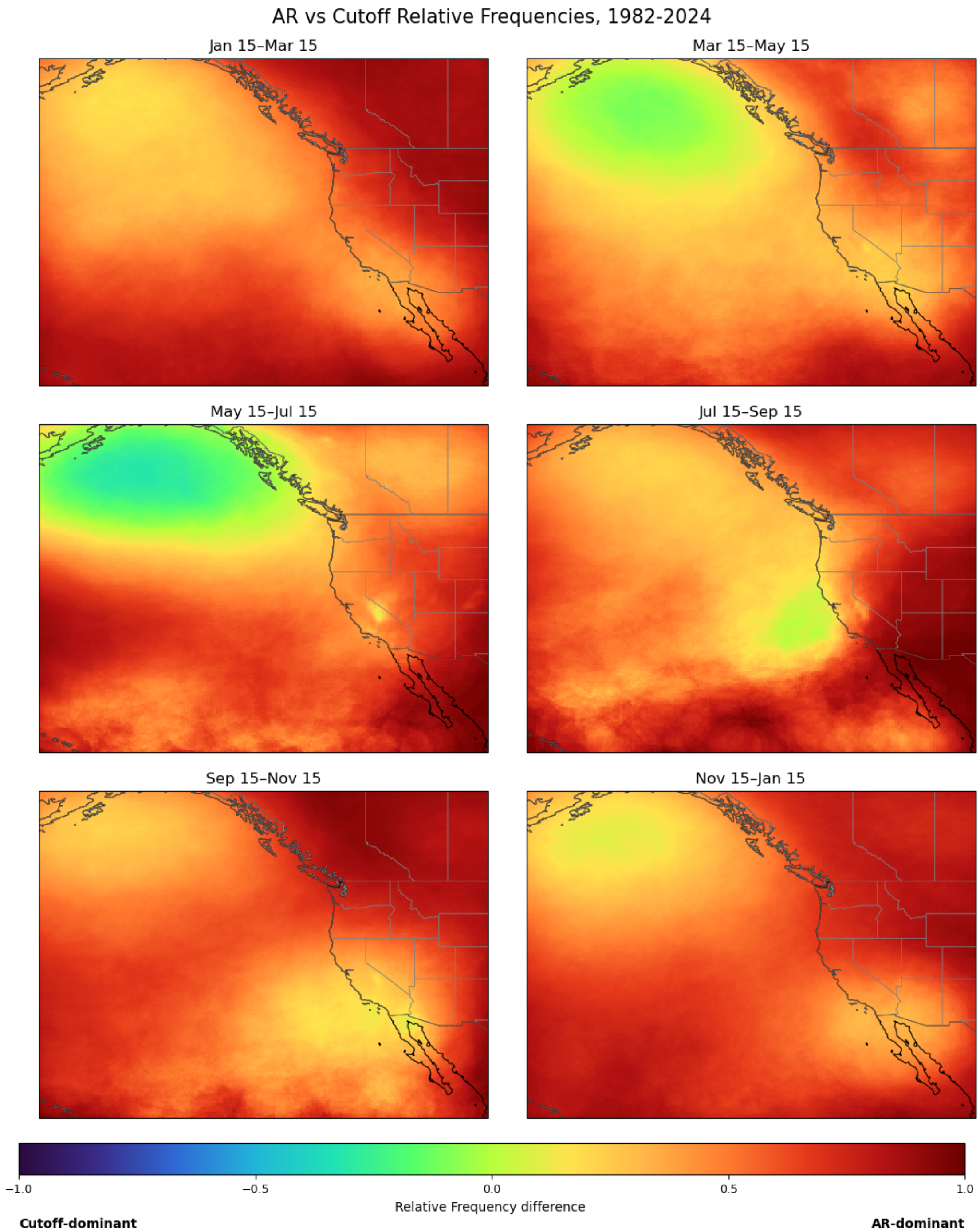

Figure 3.5: Heatmap representing cutoff low and AR seasonal relative frequencies as defined in the methods section Eq. (1). Colors closer to the blue spectrum represent cutoff low-dominant regions, and colors closer to the red spectrum represent AR-dominant regions. Relative Frequency Difference below the figure refers to the difference of spatial occurrence frequency when comparing both cutoffs and ARs on one overlapping plot.

Figure 3.5 shows the relative frequency patterns of both cutoff lows and ARs during the same 2-month periods. ARs are much more common in the PNW during mid-September to mid-March, in NorCal during mid-November to mid-January, and in SoCal during mid-July to mid-September when both systems occur infrequently. The Gulf of Alaska and SoCal regions exhibit higher numbers of cutoff low events, although the frequencies are still lower than winter AR frequencies. The Gulf of Alaska region exhibits frequent cutoff low events, with a fraction of them making their way down the California coast, as discussed earlier in the chapter. Mid-July through mid-September shows an increase in cutoff low relative frequencies in the NorCal coastal region most likely due to a sharp decrease in AR events. Lastly, from mid-November to mid-January, ARs still dominate the West Coast as a whole, but the Gulf of Alaska and SoCal regions exhibit relatively higher frequency of cutoff low activities. It is important to note that while NorCal and SoCal experience periods when cutoff low frequency nearly matches AR frequency, the PNW does not show a similar pattern. As ARs propagate farther inland, their intensity begins to diminish, especially beyond the Cascade and Sierra Nevada Mountains. Cutoff lows, specific to the West Coast, reach their highest frequencies past the coastal regions and propagate further into the interior western United States.

3.4 Summary

The figures in this chapter illustrate significant differences between ARs and cutoff lows in annual frequencies, seasonal variability, and spatial extent. While ARs dominate in both affected area and total annual frequency over the Northeast Pacific Ocean and western North America, cutoff lows tend to outnumber ARs in the Gulf of Alaska from mid-May to mid-July (Fig. 3.5). The differences in annual frequencies suggest that overall, ARs occur much more frequently and exhibit much broader spatial footprints across the Northeast Pacific Ocean and western United States. Cutoff low frequencies approach or exceed AR frequencies only from early spring through late summer. ARs are more frequent than cutoff lows during most of the year, especially in winter, whereas cutoff lows are more frequent during May to July in the Gulf of Alaska. This finding also suggests that overlapping precipitation from the two systems at the same time and location is likely much less common than precipitation associated with only one system. There are cases in the climatology when ARs and cutoff lows occur simultaneously in nearby areas (not shown), indicating that these two systems can be associated and may jointly contribute to precipitation. While their individual contributions are relevant to this study, it is important to emphasize that cutoff lows and ARs could influence one another's precipitation totals and spatial distributions.

Chapter 4 SEASONAL AND REGIONAL RELATIONSHIPS BETWEEN CUTOFF LOWS AND PRECIPITATION OVER THE U.S. WEST COAST

The three regions defined earlier in this study (PNW, NorCal, and SoCal) were selected to represent areas where precipitation contributions and event frequency display different patterns. Similar methods have been used in literature to describe AR intensities and frequency in specified regions (Ralph et al., 2019). After calculating precipitation totals for all three regions, this study examined and presented seasonal precipitation associated with cutoff lows and ARs separately for each domain.

4.1 Cutoff Low and AR Precipitation Contributions in the PNW

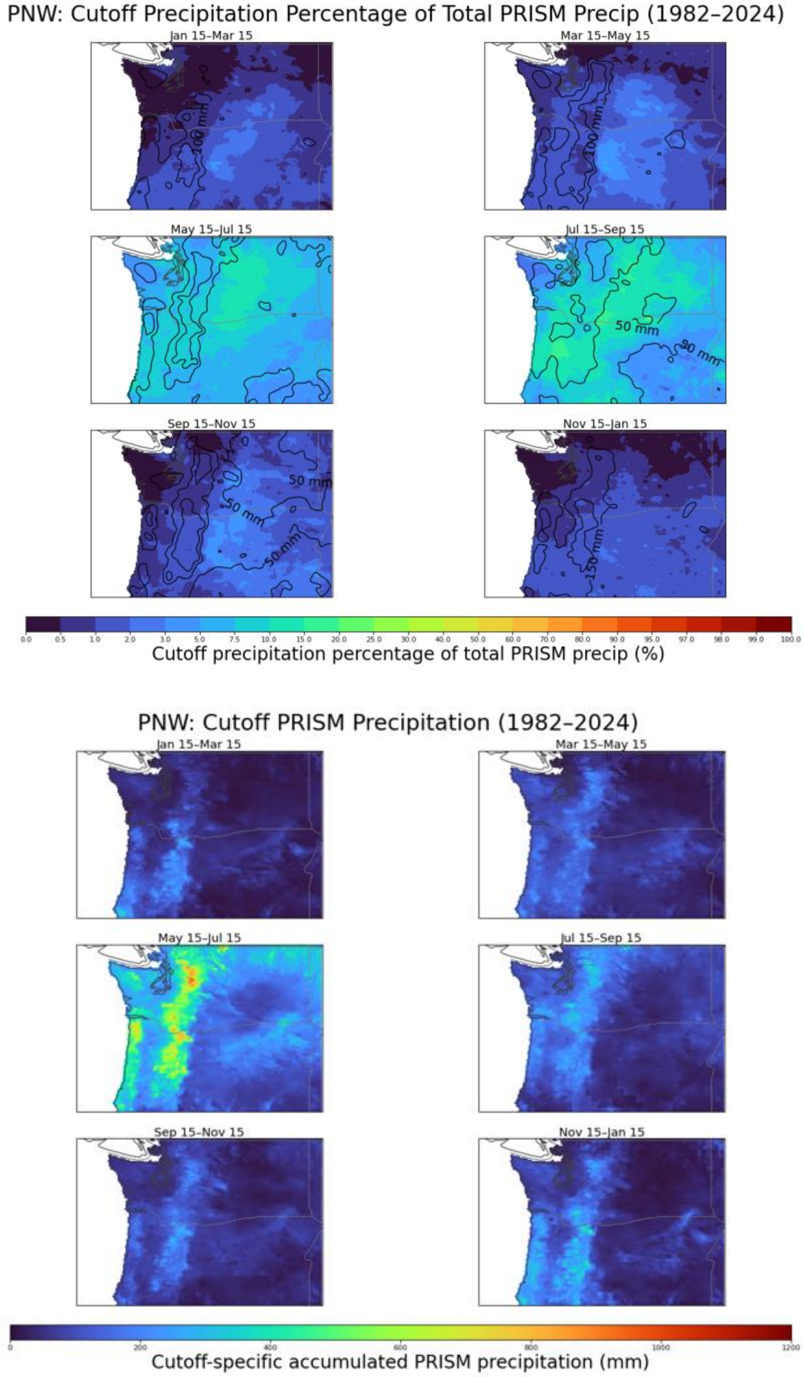

Figure 4.1: Multi-panel plots showing the seasonal contributions (percentage in color shading; absolute amounts in black contours) of total precipitation (top panel) from cutoff lows only in the PNW during 1982-2024. The black contour lines bound areas of the specified quantity of observed PRISM precipitation. The bottom panel represents the total accumulated raw PRISM precipitation values specific to cutoff low occurrences, with brighter colors representing stronger accumulations.

Figures 4.1 and 4.2 represent the seasonal cutoff low and AR precipitation percent contributions, respectively, for the PNW. In Figure 4.1, the precipitation represents only precipitation associated with cutoff lows and does not include contributions from ARs or other sources not discussed. Mid-May through mid-July has the highest percentage of precipitation associated with cutoff low events in the PNW. During these low-AR frequency months, cutoff lows contributed a maximum average of 25% of the region's precipitation and are mostly confined to areas east of the Cascades. During the fall and winter months in the PNW, the relative contribution of cutoff lows to precipitation rapidly drops, with some areas receiving as little as 1% of the accumulated total from cutoff lows.

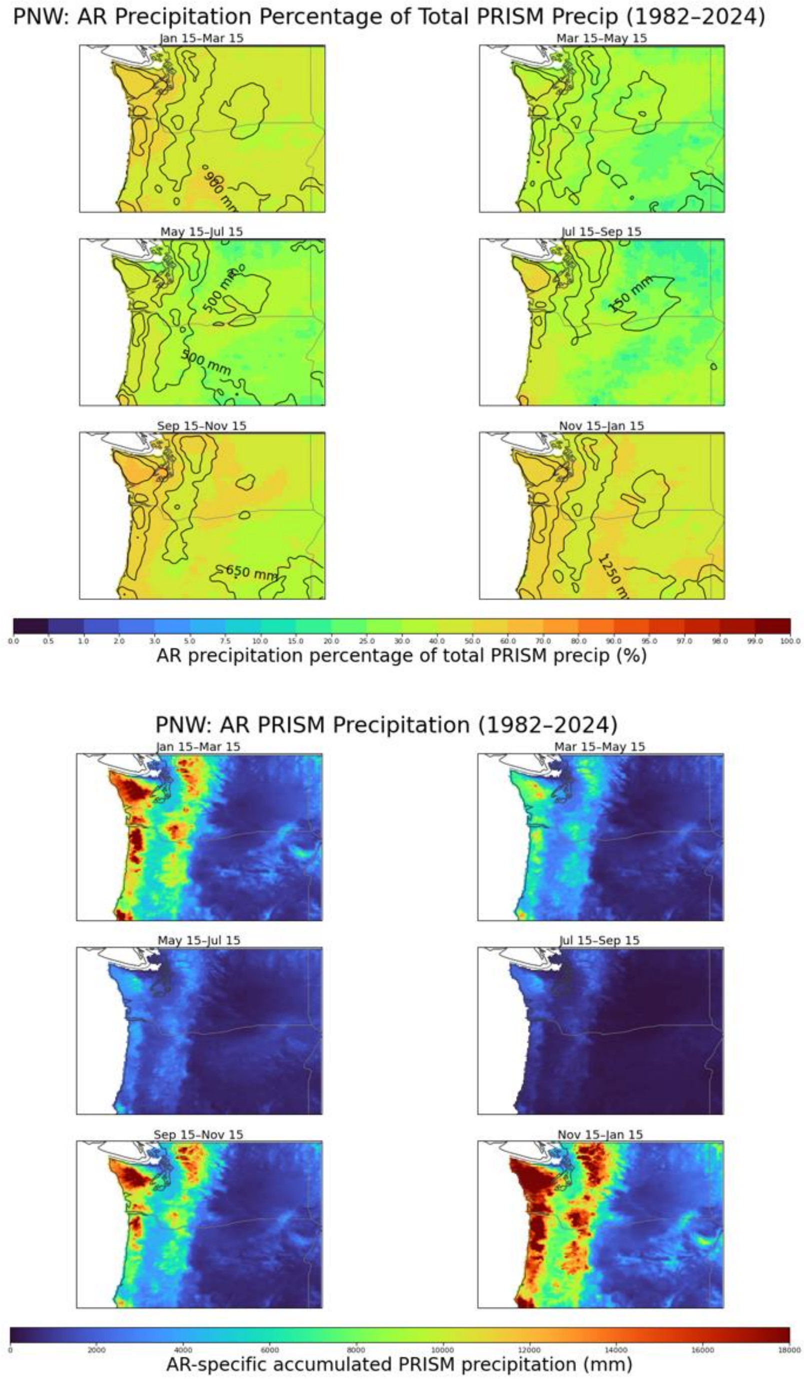

Figure 4.2: Multi-panel plots showing the seasonal contributions (percentage in color shading; absolute amounts in black contours) of total precipitation (top panel) from ARs only in the PNW during 1982-2024. The black contour lines bound areas of the specified quantity of observed PRISM precipitation. The bottom panel represents the total accumulated raw PRISM precipitation values specific to AR occurrences, with brighter colors representing stronger accumulations.

AR precipitation substantially differs from cutoff low precipitation, with the maximum contribution reaching ~60% from mid-September to mid-March (Fig. 4.2). This is the peak period for AR activity as well as the period with the lowest cutoff low frequency in the PNW. ARs generate much higher precipitation amounts in western Washington and Oregon than over the interior PNW. This pattern is consistent with the fact that moist upslope flux within ARs drives orographic precipitation on the windward side of the Pacific Coast Ranges and Cascades, leading to a significant reduction in moisture content and a rain shadow effect over the interior PNW. Precipitation from cutoff lows is less constrained by moisture and topography. Their variability lies mostly in Rossby wave breaking and planetary wave separation. ARs are more closely tied to midlatitude storm track and associated low-level jets, so their occurrence is enhanced in boreal winter when the North Pacific jet is stronger and more zonally extended (Madsen and Martin, 2023).

4.2 Cutoff Low and AR Precipitation Contributions in the NorCal

NorCal is a region where extreme precipitation can be influenced by multiple large-scale circulation patterns, highlighting the complexity of precipitation prediction in this region (Srivastava et al., 2025). This region consists of areas where weather pattern shifts (high- to low-pressure and vice versa) tend to have a greater effect on precipitation (Wahl et al., 2019). The pronounced volatility of these systems is one factor that makes precipitation prediction in NorCal difficult (Abatzoglou et al., 2016). A potential reason for this is that orographic lift tends to be stronger in winter than in late spring and early summer due to stronger low-level winds. The increased magnitude of these low-level winds helps drive ARs and their associated precipitation farther inland. In some cases, cutoff low precipitation may be enhanced by easterly upslope flow along the eastern slopes of north-south-oriented mountain ranges. Additionally, its location along the USWC introduces unique conditions as it lies in between the PNW (where heavy precipitation occurs) and SoCal (where comparatively little precipitation occurs).

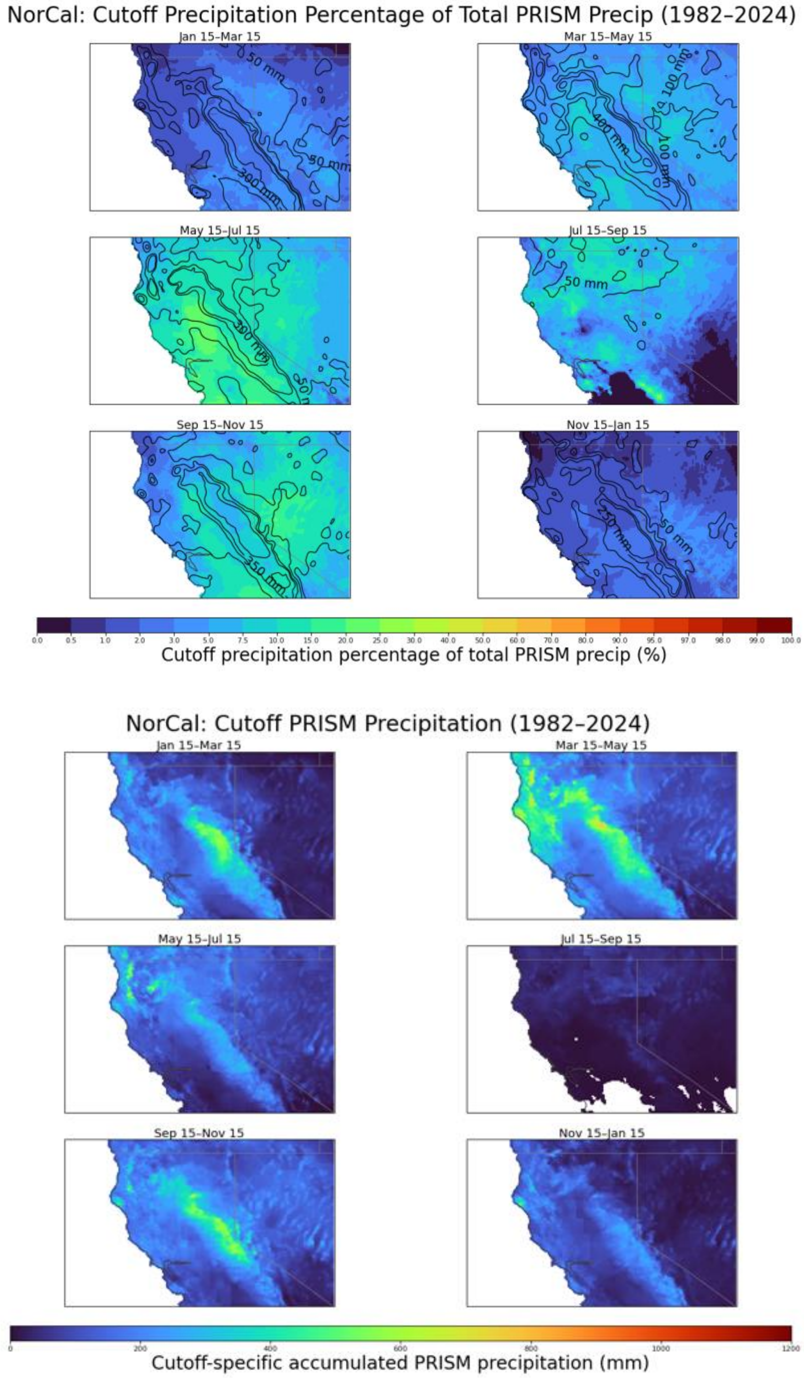

Figure 4.3: As in Figure 4.1, but for NorCal.

When examining precipitation specifically from cutoff lows, NorCal shows a similar pattern to the PNW, with higher cutoff low contributions from late spring through early summer than from late fall through late winter (Fig. 4.3). The maximum contribution percentages are designed to indicate the maximum cutoff low (or AR) spatial precipitation percentage relative to total observed precipitation for within the respective region. Higher contribution percentages mean that the specific phenomena had a higher impact on the total amount of precipitation over time. These contribution percentages help showcase the seasonal, and regional spatial spreads of each phenomenon's maximum and minimum contributions to precipitation over all years. Maximum contribution percentages from cutoff lows exceed 40% in NorCal from mid-May to mid-July, mainly in areas near coastal ranges and the Sacramento Valley. This is the same time when NorCal exhibits its driest conditions. Similar to the PNW, the NorCal region experiences local maxima in cutoff low precipitation contributions east of major mountain regions during mid-May through mid-July, specifically areas east of the Coast Ranges and Sierra Nevada.

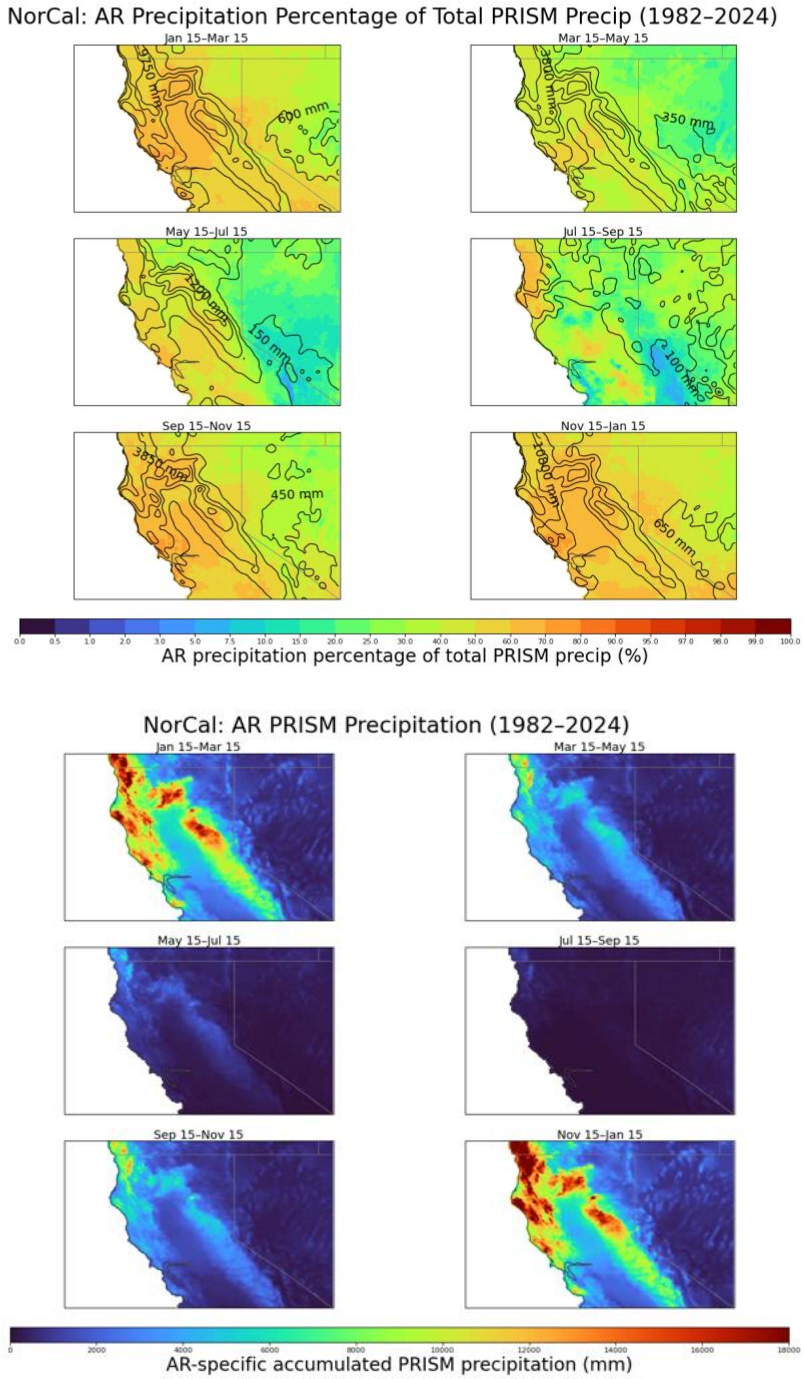

Figure 4.4: As in Figure 4.2, but for NorCal.

As shown in Figure 4.4, the AR precipitation contribution generally is larger than that of cutoff lows in NorCal. During peak AR activity months (mid-November through mid-March), the maximum percentages were consistently near or greater than 60% between the coast and the southern Cascades/Sierra Nevada. Overall, NorCal shows its largest AR precipitation contributions along the coast and in the Central Valley, while cutoff low contributions are more prevalent in the Central Valley and east of the Sierra Nevada. This pattern suggests that coastal areas within NorCal receive lower contributions from cutoff lows, but the cutoff low contributions generally increase farther inland. In contrast, AR contributions decrease farther inland as ARs become weaker and less frequent, especially from mid-May to mid-September. The Central Coast of NorCal shows signs of strong AR contributions in four out of the six monthly periods. During mid-July to mid-September, precipitation contributions from both cutoff lows and ARs show a pronounced decline in coastal areas south of Napa Valley.

4.3 Cutoff Low and AR Precipitation Contributions in the SoCal

The combination of SoCal's topography and more frequent occurrence of high-pressure ridges off the coast (Ralph et al., 2019; Srivastava et al., 2025) results in differences in precipitation in SoCal when compared to the PNW and NorCal. Several factors limit precipitation in SoCal relative to the rest of the USWC:

1) Developing troughs associated with the jet stream tend to track farther north, leaving SoCal with a higher probability of high-pressure ridges that deflect incoming Pacific storms and ARs (Ralph et al., 2019; Oakley et al., 2014).
2) Upper-level disturbances associated with the polar jet generally occur less frequently in SoCal, and when they do, they may bring colder air and relatively limited precipitation. (Baldwin et al., 2001).
3) Mountain ranges north of SoCal can make it difficult for moisture and precipitation from incoming storms to extend farther inland (Ralph et al., 2019; Srivastava et al., 2025).

Because of these constraints, SoCal has experienced severe drought years, making water resource management more challenging.

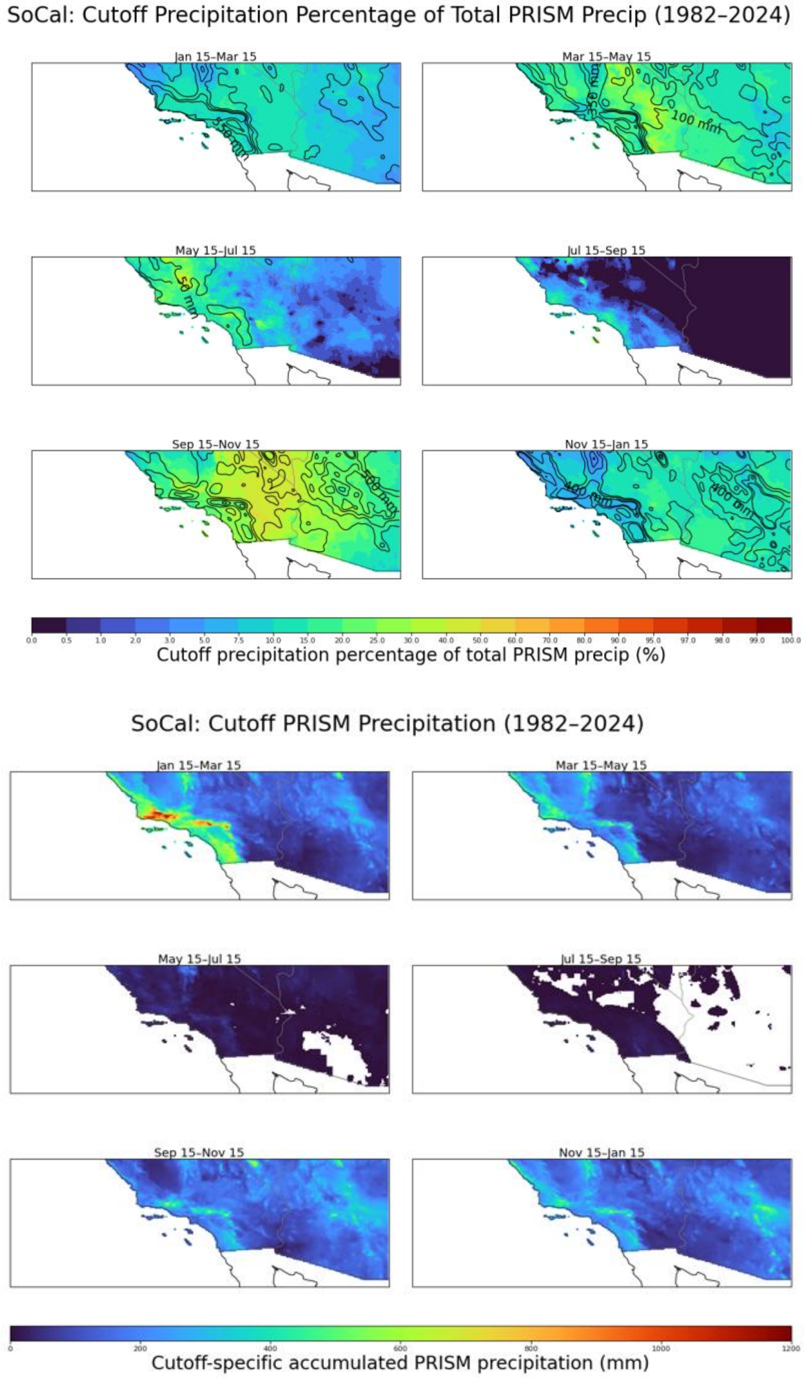

Figure 4.5: As in Figure 4.1, but for SoCal. The white areas present in SoCal's May 15 to September 15th plots are representative of areas in which cutoff low precipitation was not present (potentially due to instrumentation error), or NaN values (Not a Number) were present at this exact time and location for cutoff low precipitation.

As Figure 4.5 illustrates, the relative precipitation contributions of cutoff lows in SoCal differ significantly from other regions along the USWC. Cutoff lows contribute the highest percentage (~50-65%) of total precipitation from mid-September to mid-November. Cutoff low contributions in SoCal increase eastward from the coast toward the desert regions. This is a pattern shared by all three regions in which cutoff low precipitation contributions reach a local maximum further inland than ARs, typically on the east side of north-south oriented mountain ranges. A comparison of Figures 3.3 and 4.5 shows that cutoff lows from the Gulf of Alaska are more likely to reach SoCal during mid-September to mid-January. The figures show overall agreement in contributions and frequencies when examining the early winter months (mid-November to mid-January), where the percent contributions of cutoff lows increase as they move farther inland from the coast to the California-Arizona border. This increase in percent contributions from cutoff lows suggests seasonal variability associated with these synoptic scale events. A potential factor influencing the more eastern extent of cutoff lows is that in early winter for the USWC, colder air aloft is more present along the regions of SoCal and will promote upper-level divergence which influences the stronger instability necessary for cutoff lows to persist. Combined with the fact that ARs contribute most of their precipitation to the PNW and NorCal, we suggest that lower moisture transport to the south (SoCal) and stronger temperature gradients providing cold air aloft, result in longer-lasting cutoff lows that feed on the instability associated with SoCal in the early winter months. The minimum cutoff low precipitation contribution occurs in mid-November to mid-January in the PNW and NorCal, and the minimum in SoCal occurs in mid-July to mid-September. This mid-July to mid-September period in SoCal also coincides with the North American monsoon season, when monsoon moisture and convective thunderstorms contribute to summer precipitation across inland

Southern California and Arizona (Heintzman et al., 2022; Prein et al., 2022). These additional summer precipitation processes may reduce the relative contribution of cutoff lows to total precipitation in SoCal. Clemesha et al. (2023) showed that monsoonal moisture transported into Southern California reduces coastal low cloud cover during summer, but did not provide direct results about precipitation (Heintzman et al., 2022; Prein et al., 2022).

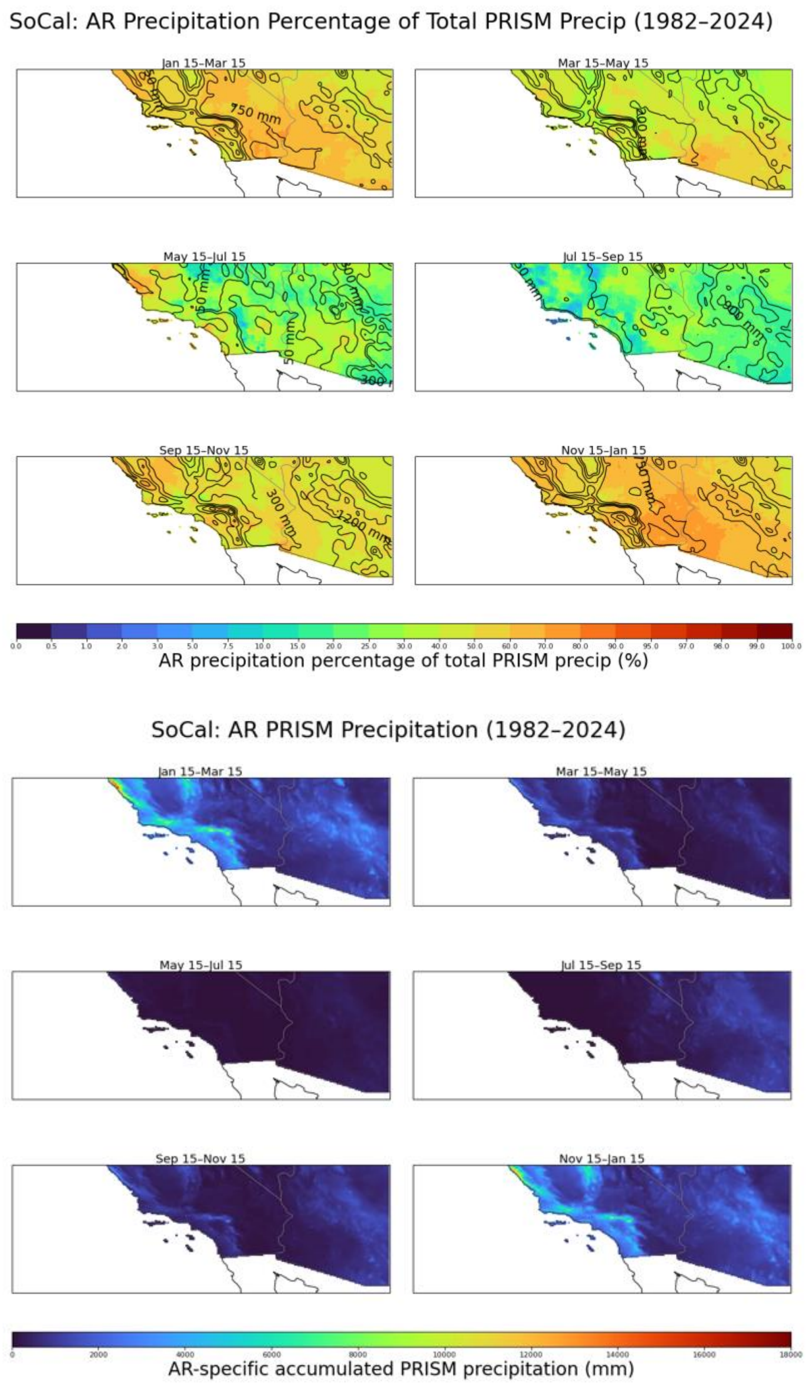

Figure 4.6: As in Figure 4.2, but for SoCal.

Seasonal precipitation contributions from ARs can often be inversely related to those from cutoff lows in SoCal, except from mid-November to mid-January (maximum), and from mid-July to mid-September (minimum) (Fig. 4.6). Maximum percentages range from ~50% to

70% from mid-November to mid-March, highlighting the seasonal increase in AR activity. Notably, when moving southward from the PNW to SoCal, ARs in early winter appear to reach farther inland. For SoCal, this is true for mid-September through mid-March, whereas NorCal and the PNW only extend inland in mid-November to mid-March on average.

4.4 Combined Regional Precipitation Patterns

All three regions experience wide ranges in precipitation percent contributions from cutoff lows, especially in NorCal. From mid-May to mid-July, NorCal experiences a minimum contribution of 3% (west of the Sierra Nevada) and a maximum of 40% (over the Sierra Nevada) from cutoff lows. In the PNW, cutoff low maximum percentages reach 25% during mid-May to mid-July (northwest and southeast region), which is 15% less than the maximum to the cutoff low contributions in NorCal. SoCal experiences the greatest seasonal and spatial variability in percent contributions from cutoff lows. Mid-September to mid-November ranges from 2% to 60%, and mid-November to mid-January ranges from 2% to 50%. When reporting contributions to precipitation from cutoff lows using observed values, we found that in the PNW from mid-May to mid-July, cutoff low precipitation varied from 200mm to 1200mm over the 42-year record (mostly east of the Cascades). NorCal had its highest accumulations of observed cutoff low precipitation from mid-March to mid-May with total variations ranging from 100mm to 800mm. SoCal had its highest amounts of observed cutoff low precipitation from mid-January to mid-March, varying from 100mm to 1200mm. When differentiating between the highest percentage of precipitation versus the actual observed precipitation we find that the PNW had its highest percentages of cutoff low precipitation from mid-May to mid-July, as well as its highest totals of observed cutoff low precipitation for the same months. As previously stated, NorCal had its highest contribution percentages of cutoff low precipitation from mid-May to mid-July, but had its largest observed precipitation from cutoff lows from mid-March to mid-May. The greatest difference between the contribution percentages to precipitation for cutoff lows against their raw observed contributions took place in SoCal, where maximum percentages from cutoff lows occurred from mid-September to mid-November, but observed precipitation from cutoff lows in SoCal was highest from mid-January to mid-March. The main finding from this study is that when we move from the PNW to SoCal, the time between cutoff low maximum percent contributions to precipitation and their actual observed accumulations to precipitation differ. These larger time differences between the maximum percent contribution and their respective observed precipitation from cutoff lows for SoCal are significant, given that NorCal and the PNW exhibit less spatial variability, suggesting that SoCal does not share the same cutoff low precipitation patterns as the other two regions. This analysis suggests that the USWC's topography can influence the spatial distribution of precipitation.

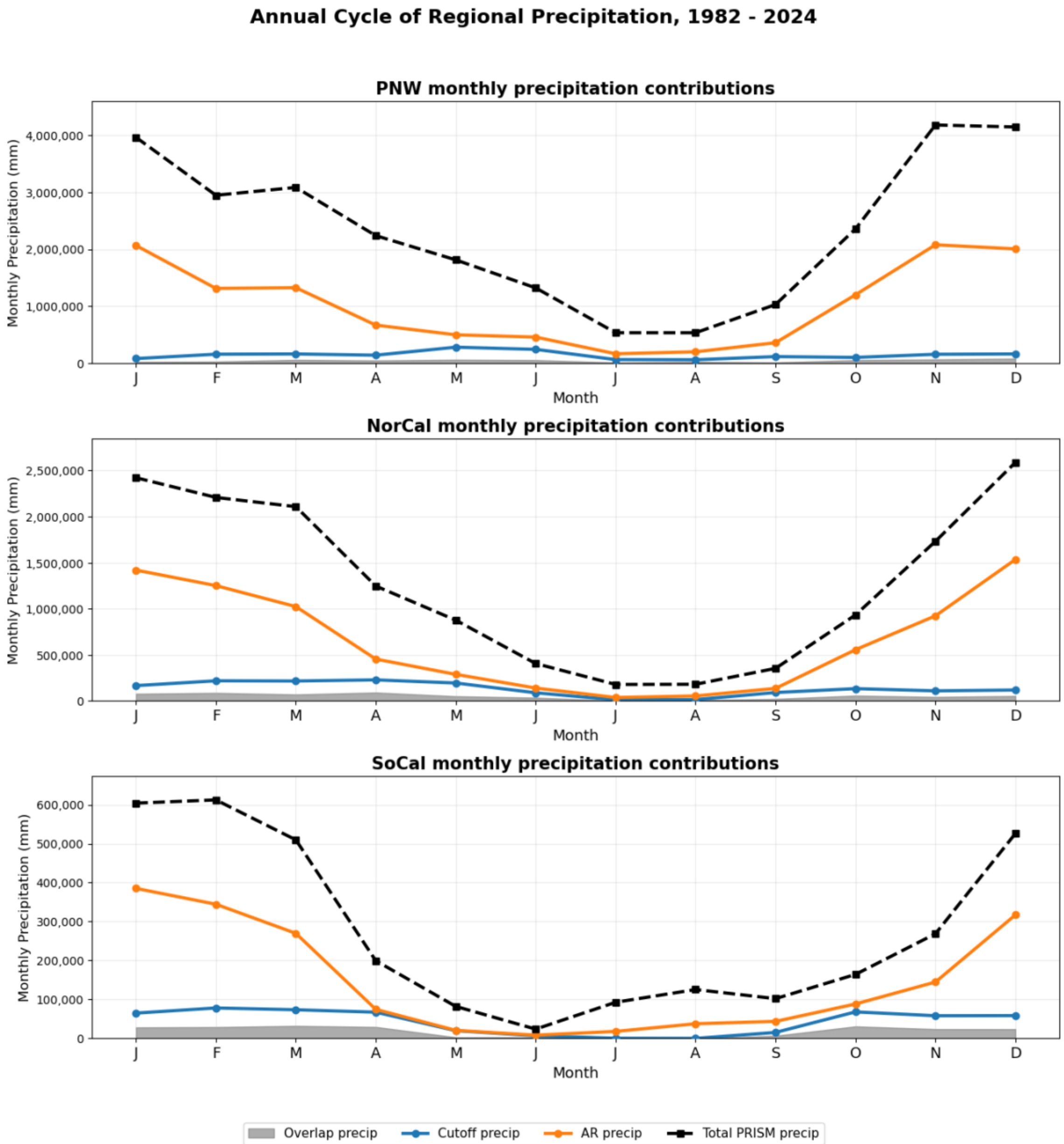

Figure 4.7: Total monthly event-based precipitation from 1982 to 2024 in the PNW (top), NorCal (middle), and SoCal (bottom). The black dashed line in each panel represents total precipitation from all sources in each region. Orange lines denote AR-only precipitation, and blue lines denote cutoff low-only precipitation. The dark grey shading indicates the total precipitation during overlapping cutoff low and AR events.

Figure 4.7 illustrates the monthly variability in regional precipitation, with each region assessed using four categories: total precipitation, AR precipitation, cutoff low precipitation, and overlapping precipitation. Precipitation was considered "overlapping" when the AR mask and cutoff low effective radius intersected and PRISM precipitation was recorded within the overlapping area. Overall, all three regions exhibited relatively small overlapping precipitation contributions. While total precipitation amounts differ significantly among the three regions, the overall seasonal cycles are similar, with a peak in precipitation during the November–March cool season. The monthly peak in precipitation occurs about two months later in SoCal (from January to February) than in the PNW (from November to December). SoCal also differs from the other two regions because precipitation increases in July–August after reaching a minimum in June, whereas precipitation reaches a minimum in July to August in the PNW and NorCal. Total precipitation generally follows similar patterns to AR precipitation. This pattern is consistent with previous findings that ARs contribute 30–45% of all USWC precipitation (Dettinger et al., 2011), with maxima consistent from November to March in all three regions. For cutoff lows, precipitation maxima occur in the PNW from May to June, in NorCal from February to May, and in SoCal from October to April, with SoCal showing the strongest maxima. The overlapping precipitation was most prevalent in NorCal and SoCal from January to April. SoCal also experienced an increase in overlapping precipitation from September to October that was not explicitly present in the NorCal region.

4.5 Summary

The results presented in Chapter 4 show a consistent pattern of ARs being the dominant precipitation source during mid-November to mid-March across all three regions, but for cutoff lows, the results are more variable. Both the PNW and NorCal regions receive a higher percentage of precipitation from cutoff lows between mid-May to mid-July, likely due to a substantial decrease in AR frequency during these months, as well as a slight increase in cutoff low frequency in spring. SoCal cutoff low contributions to precipitation are highest during mid-January to mid-March and again during mid-September to mid-November. This is in part because SoCal experiences a peak in cutoff low occurrence frequency from mid-September to mid-November, which is consistent with SoCal receiving larger precipitation contributions in the early winter months. ARs, on the other hand, contribute their largest amounts of precipitation in the PNW and NorCal from mid-November to mid-March, whereas SoCal lags a month behind from mid-November to mid-March. Lastly, the spatial variability in percent contributions to precipitation is much larger in SoCal than in the other two regions. At least 5% and at most 30% of 2-monthly precipitation (mid-May to mid-July) could be attributed to cutoff lows across the region in the PNW and NorCal. SoCal had a minimum of 0% cutoff low precipitation but a maximum of 85% from mid-May to mid-July, the largest spatial distributional difference within a 2-month time period. These results suggest that SoCal precipitation is more sensitive to cutoff lows throughout the year and that it shares only a partial relationship with the regional patterns observed in the PNW and NorCal.

Chapter 5 RESULTS AND CONCLUSIONS

This research is motivated by the need for a greater understanding of how cutoff lows contribute to precipitation in the USWC. By building a climatology of precipitation associated with cutoff lows and comparing it with the more dominant contribution from ARs, this study aims to provide watershed managers with broader knowledge of these systems and help them to better understand drought and flood risks associated with cutoff low events. Developing an initial foundation for historical cutoff low patterns and their relationship to West Coast precipitation could help to support new approaches to better predict and prepare for incoming cutoff low systems.

From 1982 to 2024, the annual frequency of cutoff lows shows a maximum of 70 days per year in the Gulf of Alaska region. Regions along the USWC (PNW, NorCal, and SoCal) experience an average of 20 cutoff low days per year, with frequencies decreasing by about half when moving further east from the coast. The annual frequency of ARs shows a broad peak over the Northeast Pacific Ocean between 45° and 55°N, with a maximum of 90 AR days per year. AR frequencies along the USWC show larger spatial variability from north to south than cutoff lows. The PNW experiences an average of 60 to 70 AR days per year, the highest frequency among the three USWC regions. NorCal shows between 50 to 65 AR days per year on average, with SoCal trailing with 45 to 50 AR days per year. AR frequency tends to decrease when moving further inland from the coastlines. The zonal gradients of AR frequency are most pronounced in the PNW. Areas within the southwestern U.S. showed signs of a weaker zonal gradient in AR frequency (Figure 2.4). AR occurrence frequency is higher in the PNW and NorCal than in SoCal, while cutoff low frequencies show weaker regional differences along the

USWC. ARs maintained a consistent spatial footprint throughout the early to late winter months, with cutoff lows exhibiting their highest frequencies from April through June.

The percent contribution of cutoff lows and ARs to precipitation was then calculated to estimate the regional cutoff low-specific and AR-specific precipitation contributions over land. Tables 5.1 and 5.2 below show the cutoff low and AR contributions to phenomena-specific precipitation from 1982 to 2024 respectively. Within these tables, only the event-specific (cutoff low or AR) precipitation was accounted for, precipitation due to other sources was not considered. A basic example of how to use information from these tables is: The PNW achieved 690 mm of cutoff low-specific precipitation (5.1) and 17,471mm of AR-specific precipitation (5.2) from the 42-year climatology. These values are to be compared to the total precipitation amounts (not event specific, but raw PRISM observations) in Table 5.3 where we see that in the PNW from 1982 to 2024, this region received 39,782mm of total precipitation. Of that total from 1982 to 2024, 690mm were received from cutoff lows, and 17,471mm were received from ARs.

Table 5.1: Spatially-Averaged Regional Total Cutoff Low Precipitation and Total Cutoff Low Precipitation Percentage. The cutoff low only precipitation (left column) shows the total amount of cutoff low-specific precipitation from 1982 to 2024. The cutoff low only precipitation percentage (right column) shows each region's percentage share of the total USWC cutoff low precipitation.

Region	Cutoff Low only Precipitation	Cutoff Low only Precipitation Percentage
PNW	690mm	26%
NorCal	890mm	33%
SoCal	1,083mm	41%

Table 5.2: Spatially-Averaged Regional Total AR Precipitation and Total AR Precipitation Percentage. The AR only precipitation (left column) shows the total amount of AR-specific precipitation from 1982 to 2024. The AR only precipitation percentage (right column) shows each region's percentage share of the total USWC AR precipitation.

Region	AR only Precipitation	AR only Precipitation Percentage
PNW	17,471 mm	49%
NorCal	12,986mm	36%
SoCal	5,385mm	15%

Table 5.3: Spatially-Averaged Regional Total Precipitation (not event-specific) from 1982 to 2024. The second column represents the total amount of all precipitation within the entirety of each region. The third column is calculated annual precipitation which can be found by using the quantities in column two and dividing them by the number of years surveyed (42 year). The last column shows the total regional percentage of the USWC precipitation.

Region	Total Precipitation over entire region(mm)	Average Annual Precipitation rate over entire region(mm/year)	Percentage of total USWC Precipitation
PNW	39,782 mm	947 mm/year	52%
NorCal	25,293 mm	602 mm/year	33%
SoCal	11,521 mm	274 mm/year	15%

The PNW had an average precipitation rate of 947 mm/year, NorCal 602 mm/year, and SoCal 274 mm/year (Table 5.3). The PNW provided 52% of all USWC precipitation from 1982 to 2024 (not specific to source of precipitation; Table 5.3). NorCal supplied 33%, and SoCal 15% of the total precipitation. Of these percentages, 4% of the precipitation occurred during cutoff low-only phenomena and 47% during AR-only occurrences, together representing 51% of total precipitation associated with either cutoff lows or ARs. ARs in the PNW and NorCal provide the largest contributions relative to the total precipitation over the USWC. The PNW and NorCal regions show similar seasonal contributions from cutoff lows and ARs, but SoCal shows a different pattern, specifically with cutoff low contributions to precipitation from mid-May to mid-July. In contrast, SoCal experiences fewer ARs (Fig. 3.2), while cutoff low occurrence frequencies are relatively comparable to those in regions farther north of USWC (Fig. 3.1). SoCal, however, has the largest percentage contribution to precipitation from cutoff lows. This may be due to the lower AR occurrence frequencies in SoCal, meaning cutoff lows can account for a larger fraction of total precipitation. All three regions share one common feature: moving southward from the PNW to SoCal, cutoff low precipitation contributions tend to increase. In the PNW, the cutoff low precipitation accounted for 2%, and ARs for about 44% of the total regional precipitation. Farther south in NorCal, both the total precipitation percentages from cutoff lows and ARs increased, while cutoff lows accounted for 4% and ARs accounted for 51% of total precipitation. SoCal had a total percentage of 9% from cutoff lows and 47% from ARs.

From 1982 to 2024, the PNW received the highest amount of precipitation (Table 5.3), but received the lowest percent contributions from cutoff low and AR-specific precipitation (Tables 5.1, 5.2). SoCal, on the other hand, received the least total precipitation (Table 5.3) but had the highest percent contributions from cutoff lows among the three regions (Table 5.1). The results show that the PNW received a total cutoff low precipitation amount of 690 mm 26% of all cutoff low-specific precipitation along the USWC), NorCal received 890 mm (33% of all cutoff low-specific precipitation), and SoCal received 1,083mm (41% of all cutoff low-specific precipitation) (Table 5.1). These values and percentages are specific to only cutoff low precipitation and does not include precipitation from any event outside of the cutoff low observational analysis.

Table 5.4: Combined Total Event-Specific Cutoff Low and AR Precipitation Amounts and Percentages from 1982 to 2024. The total precipitation (left column) is the sum of all cutoff low-specific and AR-specific precipitation in each region during 1982–2024. The total percentages (right column) indicate the combined event-specific precipitation as a percentage of total precipitation in each region across all years.

Region	**Total Precipitation Amounts (Cutoff + AR) (mm)**	**Total Percentages (Cutoff + AR)**
PNW	18,160mm	46%
NorCal	13,876mm	54%
SoCal	6,468mm	56%

While AR events historically contribute significantly to the USWC's precipitation totals, cutoff lows provide varying fractions of total precipitation, depending on season and region. Cutoff lows contribute a larger percentage of precipitation in SoCal, where AR frequencies are lower than farther north in the PNW. SoCal and NorCal received over 50% of their precipitation from the combination of ARs and cutoff lows, whereas the PNW received less than 50%. This suggests that the PNW has other important sources of regional precipitation. Splitting the analysis into three regions (PNW, NorCal, SoCal) enabled a more in-depth examination of how these events differ in overall contributions, frequencies, and historical patterns. By utilizing climatological data to present precipitation metrics, cutoff-low categorization, and AR tracking, the work sheds light on the historical relationship between cutoff lows and ARs along the USWC and their contributions to precipitation.

In this study, overlapping events are classified when an AR footprint and a cutoff low's optimal radius intersect and precipitation occurs within the overlapping area. It is important to note that while an AR and cutoff low may occur simultaneously, the spatial footprints used to calculate precipitation from ARs and cutoff lows may introduce uncertainty into the attribution of precipitation. The detected AR objects typically cover relatively larger areas, which could lead to more precipitation being attributed to ARs than to cutoff lows. Cutoff lows may also be influenced by synoptic scale dynamical processes that extend beyond the area of their effective radius. Therefore, cutoff low contributions to precipitation might be underestimated because precipitation associated with surrounding synoptic-scale processes may occur outside the defined optimal radius. Cutoff lows and ARs are sometimes present during the same precipitation events, but while they may influence one another over time, the direct spatiotemporal overlap between the two is relatively rare (see Appendix A).

Future research into this topic could help further evaluate historical cutoff low precipitation events beyond the USWC and affect the midwestern and east coast areas of the U.S. Midwestern cutoff lows (depending on the season) have historically been associated with tornados and other mesoscale convective features such as supercells and hail events (Kasuga et al., 2021). These smaller mesoscale events introduce large uncertainties in weather forecasting, partly due to a cutoff low's stationary nature (Oakley and Redmond, 2013), as discussed in the introduction. Seasonal cutoff low precipitation relationships have been discussed in midwestern areas such as the Great Lakes (Abatzoglou, 2016), but long-term pattern analysis may be needed to better quantify their overall contributions to precipitation in the Midwest and eastern regions. Similarly, cutoff lows have also been assessed in Atlantic regions and across southern Europe (Nieto et al., 2005) to better understand the duration and downstream effects of these low-pressure systems. The previous cutoff low catalogs have addressed questions regarding precipitation within their specific regions while also providing future guidance for future studies of these phenomena. Another avenue of cutoff low research relies on assessing their economic, socioeconomic, and flooding impacts. Previous assessments for ARs and their economic impacts were estimated $50.8 billion in flood damages across 11 western conterminous states over a 40-

year period (Corringham et al., 2019). Future work includes determining how cutoff lows evolve as they move further inland and away from the USWC, especially when considering ARs often weaken rapidly after landfall along major coastlines. Many questions remain for the cutoff lows. How often does a closed low separate from the main jet stream to form a cutoff low? Do these frequencies change depending on the season? Do the East and West coasts share similar patterns in the overall precipitation contributions? Research into these questions would present valuable pathways for forecasters and water managers, and ultimately, improve our understanding of how to evaluate cutoff lows in future research.

Appendix A: EFFECTIVE RADIUS DISCUSSION

Determining the location and effective radius of cutoff lows is crucial for better understanding their contributions to precipitation. This analysis consisted of utilizing the Lupo and Schwartz, 2025, cutoff low catalog and testing the sensitivity of the estimated precipitation from a cutoff low when the effective radius changes.

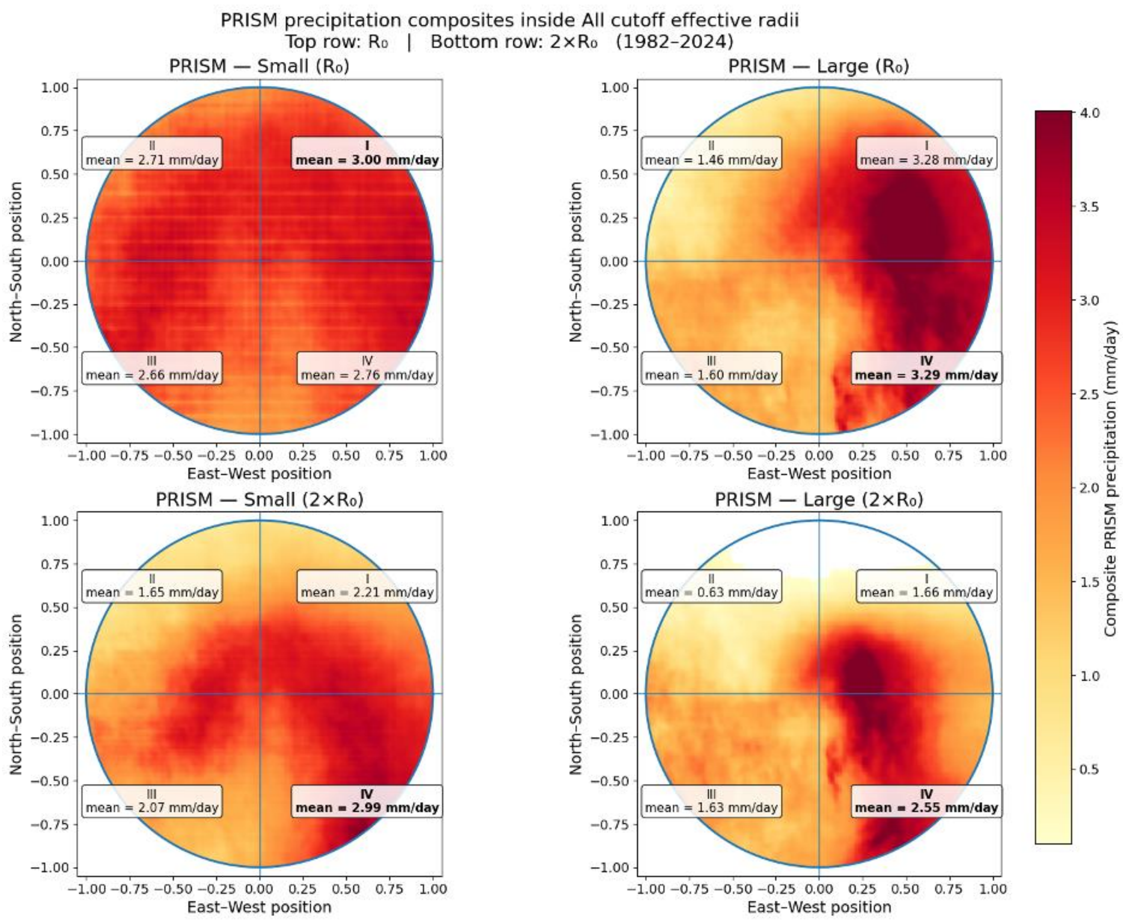

Figure A.1: Top: average precipitation intensity (color shading; mm per day) within the optimal radius of cutoff lows with small radius (<500 km; top left) and large radius (>500 km; top right) during 1982-2024. Bottom; Same analysis based on a doubling of the radius in cutoff lows with small (bottom left) and large (bottom right) radius. Each quadrant (I-IV) represents a different region of the precipitation within the effective radius. Darker red indicates areas with higher precipitation amounts, whereas lighter orange and yellow colors indicate areas with lower precipitation amounts.

Figure A.1 shows the composite mean distribution of precipitation within a cutoff low on all cutoff low days from 1982 to 2024. The left-most plots represent when a cutoff low's effective radius is small (effective radius is $R_o < 500$ km), and the right-most plots when a cutoff low's optimal slope is large (effective radius is $R_o \geq 500$ km). These composites only take into account cutoff low events that produce precipitation over land and consist of more than 0.1 mm of rainfall in a given day. The plots on the bottom row show the same analysis, but with the effective radius being doubled from its original values found in the catalog. By doubling the effective radius of the cutoff lows, we can examine surrounding precipitation that might not have been accurately awarded to a cutoff low system.

The plots in the top row indicate that the largest average precipitation falls within quadrant I for $R_o< 500$ km and quadrants I and IV for $R_o > 500$ km. Both are on the eastern side of the cutoff low's circular area, which supports the idea that moisture advection and precipitation-producing features are more likely to occur on the eastern side of a cutoff low. A smaller effective radius shows more evenly distributed precipitation within the cutoff low, and larger effective radius show more centralized features in the eastern quadrants. The spread of mean quadrant values is also wider for larger cutoff lows, where the western quadrants (quadrants II and III) average roughly 1.5 mm/day inside the effective radius, and the eastern quadrants average approximately 3.3 mm/day.

We next consider the sensitivity of the precipitation distribution within the cutoff low to a theoretical doubling of the effective radius. When doubling the effective radius of the smaller cutoff lows (bottom left panel of Figure A.1), the PRISM precipitation maximums were more organized in a contained area. The increase in effective radius allowed for better visual representation of where precipitation most likely occurred when inside a small cutoff low's effective radius. For the larger cutoff lows (bottom right panel), doubling the effective radius confirms that the easternmost quadrants of a cutoff low receive the largest composite precipitation.

When comparing the top and bottom rows of Fig. A.1, the rightmost plots (larger radius) show that across the entire climatology, most of the precipitation within a cutoff low's effective radius occurs in quadrant IV (the southeastern quadrant), followed by quadrant I (the northeastern quadrant). The leftmost plots, however, show that for smaller effective radius, quadrants I and IV have similar average precipitation, with a difference of 0.24 mm/day in the eastern areas (QI = 3.00 mm/day and QIV = 2.76 mm/day). When we double the effective radius, we find that QIV = 2.99 mm/day of precipitation and QI = 2.21 mm/day for the smaller-radius cases. The total difference between the northeastern (QI) and southeastern (Q2) quadrants is 0.78 mm/day, which is ~30% higher than the observed precipitation difference for the original effective radius (left-side panels of Figure A.1). This suggests that the contribution to precipitation from cutoff lows might be underestimated for effective radius below 500 km. Uncertainty in the representation of the surrounding synoptic-scale circulation may help explain why precipitation contributions from small cutoff lows are sensitive to the choice of effective radius. Lupo and Schwartz (2025) showed that GFS forecasts can exhibit overly progressive cutoff lows because of errors in the surrounding geopotential height and wind fields. Similar uncertainties in the evolution and position of cutoff lows could affect the spatial relationship between the identified cutoff low and nearby moisture and precipitation, causing some associated precipitation to occur outside the defined effective radius.

Appendix B: ALTERNATIVE SEASONAL ANALYSIS

In Chapter 3, we compared the seasonal occurrence frequency of cutoff lows and ARs by dividing the year into two-month periods. Figure 3.5 shows a heatmap of that analysis. Here, we present heatmaps for alternative three-month periods, December to February (DJF), March to May (MAM), June to August (JJA), and September to November (SON), to test the sensitivity of the results to the choice of time period.

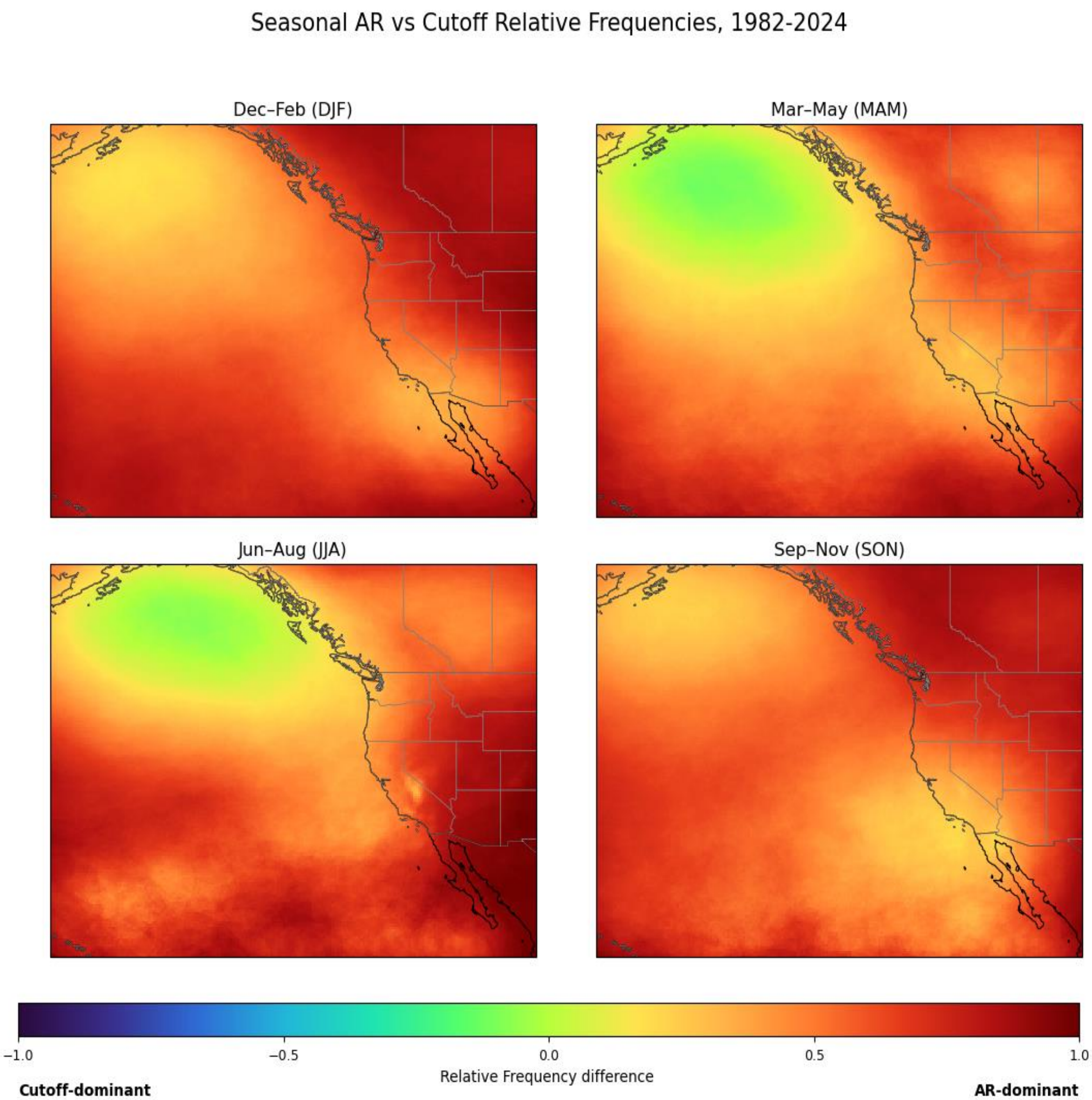

Figure B.1: Heatmap showing cutoff low and AR seasonal relative frequencies using three-month periods rather than the two-month periods shown in Figure 3.5.

Figure B.1 shows the relative frequencies of cutoff lows and ARs over DJF, MAM, JJA, and SON and represent broader seasonal changes than the two-month periods in Chapter 3. The relative cutoff low occurrence is highest during MAM and JJA in the Gulf of Alaska, consistent with Figure 3.5, which showed the highest relative cutoff low occurrence in mid-May to mid-July. The March–August period indicates an increase in cutoff low frequency in this region, whereas in Figure 3.5, the only cutoff low-dominant period was during the months of mid-May to mid-July.

Cutoff low frequency in Figure B.1 also indicates a lower cutoff low occurrence frequency near the NorCal coast from June to August, whereas Figure 3.5 shows a maximum in relative frequency from mid-July to mid-September. Changing the averaging period appears to show sensitivity in the frequencies of cutoff lows and may require further analysis. Another potential caveat to the differences in the averages comes from the fact that Figure 3.5 is shows data that starts on the 15th day of the month rather than the 1st of the month as shown in Figure B.1. Overall, the different averaging periods did not show substantial differences to the results when compared to the results of chapter 3. While the standard meteorological months are useful, we here do not use traditional three-month averages and focus on mid-monthly observations to better encapsulate seasonal pattern shifts in the precipitation. The 3-month average plot (Figure B.1) appears to smooth out the smaller scale features that are evident in Figure 3.5.

Appendix C: MONTHLY PRECIPITATION PATTERNS

The USWC historically experiences more precipitation during the late winter and early spring months. Specifically, from October to March, ARs produce substantial precipitation across all regions. The largest percent contributions of all AR-specific precipitation over the USWC occurs from October to March. Cutoff lows, however, produce their peak precipitation in March and October.

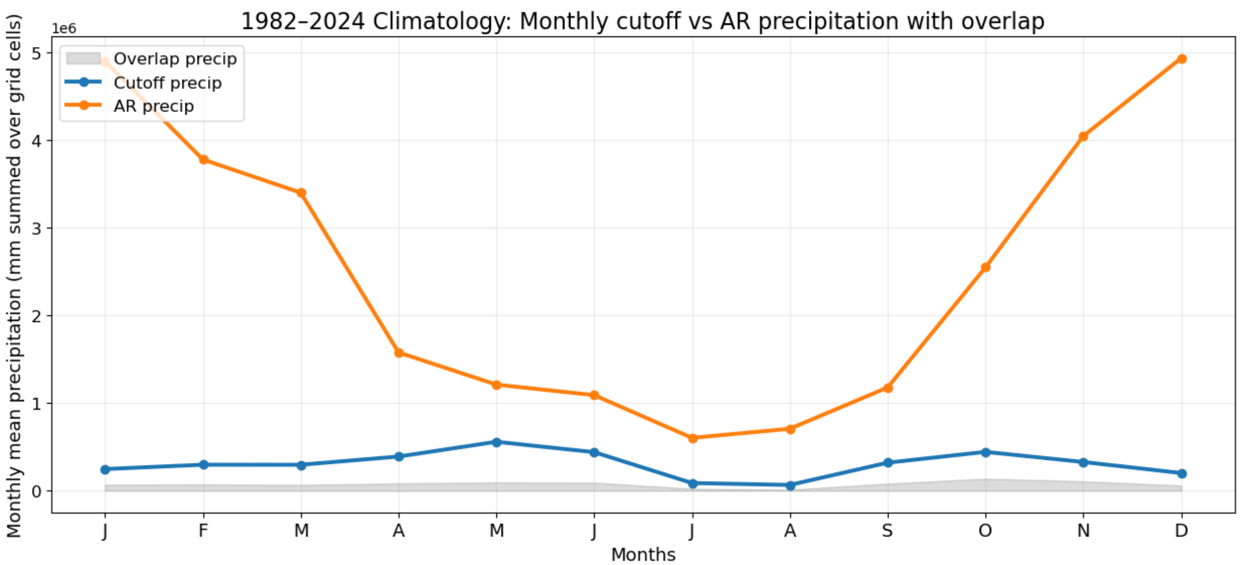

Figure C.1: Monthly mean precipitation from cutoff lows and ARs over the entire USWC. The orange line represents AR-only precipitation, the blue line represents cutoff low-only precipitation, and the gray shading represents overlapping precipitation from both ARs and cutoff lows.

Precipitation from ARs vary throughout the year, whereas cutoff low precipitation is of similar magnitude year-round. Figure C.1 demonstrates the clear dominance of AR precipitation and suggests that seasonal differences strongly influence total event-based precipitation totals. ARs produce their highest contributions in January and December, with their lowest contribution in July. Cutoff lows produce their peak contributions during May and October and their smallest contributions in July and August. Precipitation from cutoff lows and ARs is most similar from April to September. AR precipitation drops sharply from March to April, reaching a minimum in

July. Cutoff low precipitation gradually increases through spring, peaking in May, and then decrease again during summer.

From September to December, AR precipitation increases rapidly, then decreases from January to April. Cutoff low precipitation increases from August to October, but then decreases from October to January before increasing again during late winter. It isn't until May that the cutoff lows and ARs share similar trends in precipitation. May to July showed similar decreases in precipitation for both ARs and cutoff lows, suggesting that the relationship between cutoff lows and ARs are most similar during this three-month period. This could be due to both cutoff lows and ARs reaching their minimum frequency over most of the USWC during late spring and summer. With ARs less frequent in the summer months, cutoff lows may have greater potential to provide a larger contribution to the total precipitation for the USWC. The overlapping precipitation amounts were relatively low throughout the climatology. This can most likely be attributed to the fact that the AR footprint and effective radius of a cutoff low intersect infrequently over land.

REFERENCES

Abatzoglou, J.T. 2016. Contribution of Cutoff Lows to Precipitation across the United States. American Meteorological Society., 893-899 doi: https://doi.org/10.1175/JAMC-D-15-0255.1

Baldwin, M.P., Dunkerton, T.J. 2001.Stratospheric Harbingers of Anomalous Weather Regimes. Science. Vol 294, Issue 5542, 581-584. doi: 10.1126/science.1063315

Bell, G.D., Bosart, L.F. 1989. A 15-Year Climatology of Northern Hemisphere 500 mb Closed Cyclone and Anticyclone Centers. American Meteorological Society. Vol 117, 2142-2163. doi: https://doi.org/10.1175/1520-0493(1989)117<2142:AYCONH>2.0.CO;2

Cehak, K. (1971). Review Atmospheric circulation systems: PALMÉN, E. and C.W. NEWTON (1969): Their Structure and Physical Interpretation 603 pp., 250 figs., 23 tables. International Geophysics Series, vol. 13. New York/ London: Academic Press. $ 26.00. *Geoforum, 2*, 90.

Clemesha, R.E., Iacobellis, S.F., Gershunov, A., Cayan, D.R., Small, I.J., Cavazos,T. 2023. North American Monsoon Impacts Southern California's Coastal Low Clouds. Advancing Earth and Space Sciences. Vol 50, Issue 12. doi: https://doi.org/10.1029/2022GL102059

Collow, A.B., Mersiovsky, H., Bosilovich, M.G. 2020. Large-Scale Influences on Atmospheric River-Induced Extreme Precipitation Events along the Coast of Washington State. American Meteorological Society. 2139-2156. doi:https://doi.org/10.1175/JHM-D-19-0272.1

Corringham, T.W., Ralph. M.F., Gershunov, A., Cayan, D.R., Talbot, C.A. 2019. Atmospheric Rivers Drive Flood Damages in the Western United States. Science Advances. Vol 5, Issue 12. doi:10.1126/sciadv.aax4631

Davies, J. M. (2006). Tornadoes with Cold Core 500-mb Lows. Weather and Forecasting, 21(6), 1051-1062. https://doi.org/10.1175/WAF967.1

Dettinger, M. D., Ralph, F. M., Das, T., Neiman, P. J., & Cayan, D. R. (2011). Atmospheric Rivers, Floods and the Water Resources of California. *Water*, *3*(2), 445-478. https://doi.org/10.3390/w3020445

Guan B, Waliser DE. 2015. Detection of atmospheric rivers: Evaluation and application of an algorithm for global studies. Journal of Geophysical Research: Atmospheres. 120(24):12514–12535. doi:https://doi.org/10.1002/2015jd024257.

Guan B, Waliser DE. 2024. A Regionally Refined Quarter-Degree Global Atmospheric Rivers Database based on ERA5. Sci Data 11, 440 (2024). https://doi.org/10.1038/s41597-024-03258-4

Heintzman, R., Balling Jr, R. C., & Cerveny, R. S. (2022). Desert Climate Regionalization for Joshua Tree National Park and Surrounding Areas Using New Climate Network Observations. *Journal of Applied Meteorology and Climatology*, *61*(1), 13-23.

Hersbach, H., and Coauthors, 2020: The ERA5 global reanalysis. Quarterly Journal of the Royal Meteorological Society., 146, 1999-2049, doi:10.1002/qj.3803.

Hoskins, B.J., McIntyre, M.E. and Robertson, A.W. (1985), On the use and significance of isentropic potential vorticity maps. Q.J.R. Meteorol. Soc., 111: 877-946. https://doi.org/10.1002/qj.49711147002

Hirota N, Takayabu Y, Kato M, Arakane S. 2016 March. Roles of an Atmospheric River and a Cutoff Low in an Extreme Precipitation Event in Hiroshima on 19 August 2014. American Meteorological Society. doi: https://doi.org/10.1175/MWR-D-15-0299.1

Kasuga S, Honda M, Ukita J, Yamane S, Kawase H, Yamazaki A. 2021 Jun 22. Seamless Detection of Cutoff Lows and Preexisting Troughs. Monthly Weather Review. doi:https://doi.org/10.1175/mwr-d-20-0255.1.

Lupo KM, Schwartz CS, Romine GS. 2023. Displacement Error Characteristics of 500-hPa Cutoff Lows in Operational GFS Forecasts. Weather and Forecasting. 38(10):1849–1871. doi:https://doi.org/10.1175/waf-d-22-0224.1.

Lupo KM, Schwartz CS. 2025. Environmental Conditions and Forecast Error Evolution Associated with Synoptic Progressiveness Errors in GFS Forecasts. American Meteorological Society. doi:https://doi.org/10.1175/WAF-D-24-0137.1.

Ndarana, T. and Waugh, D.W. (2010), The link between cut-off lows and Rossby wave breaking in the Southern Hemisphere. Q.J.R. Meteorol. Soc., 136: 869-885. https://doi.org/10.1002/qj.627

Nieto, R., Gimeno, L., Torre, L., Ribera, P., Gallego, D., Garcia-Herrera, R., Garcia, J.A., Nunez, M., Redano, A., Lorente, J. 2005. Climatological Features of Cutoff Low Systems in the Northern Hemisphere. American Meteorological Society. 3085-3103. doi: https://doi.org/10.1175/JCLI3386.1

Oakley NS, Redmond KT. 2014. A Climatology of 500 hPa Closed Lows in the Northeastern Pacific Ocean, 1948-2011. American Meteorological Society. doi:https://doi.org/10.1175/JAMC-D-13-0223.1

Oakley NS., Orla-Barlie M., Hatchett B., Burgess P., Ralph M. 2020. Characteristics and Impacts of the April 4-11 2020 Cutoff Low Storm in California. Center For Western

Weather and Water Extremes. https://cw3e.ucsd.edu/characteristics-and-impacts-of-the-april-4-11-2020-cutoff-low-storm-in-california/

Parker, L.E. and Abatzoglou, J.T. (2016), Spatial coherence of extreme precipitation events in the Northwestern United States. Int. J. Climatol., 36: 2451-2460. https://doi.org/10.1002/joc.4504

Prein, A. F., Towler, E., Ge, M., Llewellyn, D., Baker, S., Tighi, S., & Barrett, L. (2022). Sub-seasonal predictability of North American monsoon precipitation. *Geophysical Research Letters*, *49*(9), e2021GL095602.

PRISM Climate Group. 2008. PRISM gridded climate data. Oregon State University. doi: https://doi.org/10.1002/joc.1688.

Ralph KM., Dettinger MD., Cairns MM., Galarneau TJ., Eylander J. 2018. Defining "Atmospheric River": How the Glossary of Meteorology Helped Resolve a Debate. American Meteorological Society. doi: https://doi.org/10.1175/BAMS-D-17-0157.1

Ralph MF, Rutz JJ, Cordeira JM, Dettinger M, Anderson M, Reynolds D, Schick LJ, Smallcomb C. 2019 February. A Scale to Characterize the Strength and Impacts of Atmospheric Rivers. American Meteorological Society. doi:https://doi.org/10.1175/BAMS-D-18-0023.

Singleton, A. T., & Reason, C. J. C. (2007). A Numerical Model Study of an Intense Cutoff Low Pressure System over South Africa. Monthly Weather Review, 135(3), 1128-1150. https://doi.org/10.1175/MWR3311.1

Srivastava AK, Grotjahn R, Rhoades AM, Ullrich PA. 2025. Large-Scale Statistically Meaningful Patterns (LSMPs) Associated With Precipitation Over Northern California. Advancing Earth and Space Sciences. doi: https://doi.org/10.1029/2024JD041307

Wahl, Eugene R., Zorita, Eduardo., Trouet, Valerie., Taylor, Alan H. 2019. Jet Stream Dynamics, Hydroclimate, and fire in California from 1600 CE to Present. National Oceanic and Atmospheric Administration. doi: https://doi.org/10.1073/pnas.1815292116

Zhu, Y., Newell, R.E. 1994. Geophysical Research Letters: Atmospheric Rivers and Bombs. Advancing Earth and Space Studies. Vol 21, Issue 18. doi:https://doi.org/10.1029/94GL01710

Zhu, Y., Newell, R.E. 1998. A Proposed Algorithm for Moisture Fluxes from Atmospheric Rivers. American Meteorological Society. 725-735. doi:https://doi.org/10.1175/1520-0493(1998)126<0725:APAFMF>2.0.CO;2

Zhang, Z., Ralph, F. M., & Zheng, M. (2019). The relationship between extratropical cyclone strength and atmospheric river intensity and position. *Geophysical Research Letters*, *46*(3), 1814-1823.

Zhang, Z., & Ralph, F. M. (2021). The influence of antecedent atmospheric river conditions on extratropical cyclogenesis. *Monthly Weather Review*, *149*(5), 1337-1357.